Supplementary Information

# Programmable Assembly/Disassembly of Metal-Organic Cage Integrated 2D Nanosheets

Vellaiyadevan Sivalingam[a] and Dillip Kumar Chand *[a]

[a]*IoE Center of Molecular Architecture, Department of Chemistry, Indian Institute of Technology Madras, Chennai 600036, India*

## 1. Materials and Instruments

All the commercial reagents were used without further purification unless stated otherwise. The ligands **L7**, **L8** and **L9** were purchased from commercial sources. The reported ligands **L1**, **L3**, **L4**, **L5** and **L10** were synthesized based on the reported procedures.[1–4] The new ligands **L2** and **L6** were synthesized according to the modified synthetic procedures.

NMR spectra were recorded in Bruker AV400 and AV500 spectrometers. Chemical shifts were referenced to residual solvent signals. High-resolution (ESI) mass spectra were recorded in the Agilent Q-TOF spectrometer. Rheology measurements were conducted in Anton Paar Physica MCR 301 Rheometer equipped with a cone-shaped parallel plate. Strain sweep measurements were carried out at a constant frequency of 1 rad $s^{-1}$ in the 0.1–100% range. Frequency sweep measurements were carried out at a constant strain of 5% in the 0.1–100 rad $s^{-1}$ range. High-resolution scanning electron microscopy (HR-SEM) analysis was conducted in the FEI-Quanta FEG 200F instrument. High-resolution transmission electron microscopy (HR-TEM) analysis was performed in a Technai G2 T20 instrument.

## 2. Synthesis and Characterization

### Synthesis of ligand L2

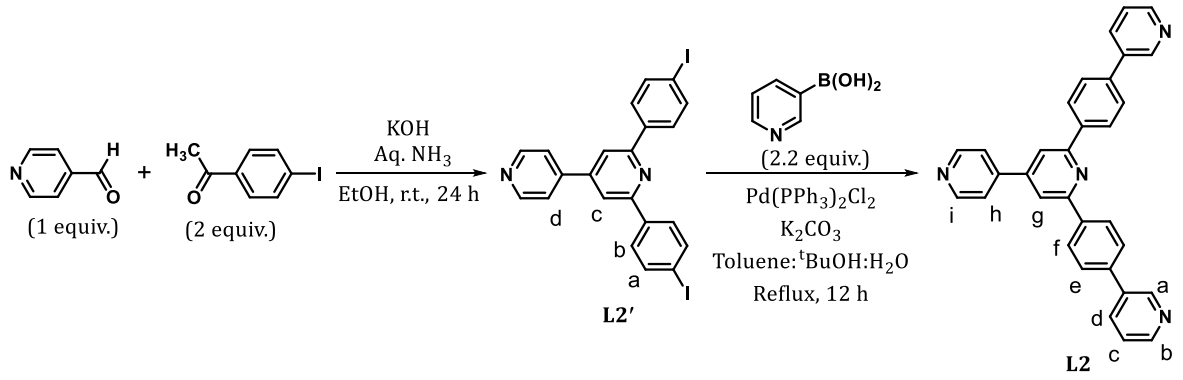


**Scheme S1** Synthesis of ligand **L2**

The new ligand **L2** was successfully synthesized in two steps, as follows:

Step I: Compound **L2′** was prepared by a modified synthetic procedure (Wang and Hanan, 2005). Pyridine-4-carboxaldehyde (0.47 mL, 5 mmol) and 4′-iodoacetophenone (2.46 g, 10 mmol) were stirred in 40 mL of ethanol. Subsequently, KOH (0.7 g, 12.5 mmol) and

aqueous $NH_3$ was added. Then, the reaction mixture was stirred for 24 hours at room temperature. The obtained precipitate was filtered and washed thrice with ethanol (3 x 10 mL). The resultant compound **L2′** (2,6-bis(4-iodophenyl)-4,4'-bipyridine) was obtained as a white solid (1.31 g, 47%) after a flash column chromatography purification (EtOAc:Hexane).

$^1$H NMR (400 MHz, 298 K, $CDCl_3$): δ (ppm) 8.78 (d, *J* = 4.7 Hz, 2H, $H_e$), 7.91–7.84 (m, 10H, $H_a$, $H_b$, $H_c$), 7.61 (d, *J* = 4.8 Hz, 2H, $H_d$).
$^{13}$C NMR (100 MHz, $CDCl_3$): δ (ppm) 157.0, 150.7, 147.8, 146.1, 138.3, 138.0, 128.8, 121.6, 116.7, 96.0.

Step II: Compound **L2′** (0.56 g, 1 mmol), pyridine-3-boronic acid (0.27 g, 2.2 mmol), $Pd(PPh_3)_2Cl_2$ (0.14 g, 0.2 mmol) and $K_2CO_3$ (0.35 g, 2.5 mmol) were taken in a double-neck round bottom flask. The reaction flask was fitted with a reflux condenser. Then, it was evacuated and purged with $N_2$, thrice in the Schlenk line. Subsequently, 35 mL of degassed toluene:water:*t*-butanol (3:3:1) mixture was added and. The reaction mixture was heated at 80 °C for about 12 hours. An excess of dichloromethane (60 mL) was added to the reaction mixture. The organic layer was extracted using DCM several times. The collected organic layer was evaporated in *vacuo,* and the product (**L2**) was purified by column chromatography (DCM:MeOH) as an off-white solid (0.39 g, 69%).

**L2**: $^1$H NMR (400 MHz, 298 K, DMSO-$d_6$): δ (ppm) 9.02 (s, 2H, $H_a$), 8.79 (d, *J* = 4.0 Hz, 2H, $H_i$), 8.62 (d, *J* = 2.9 Hz, 2H, $H_b$), 8.52 (d, *J* = 7.9 Hz, 4H, $H_f$), 8.42 (s, 2H, $H_g$), 8.21 (d, *J* = 8.0 Hz, 2H, $H_d$), 8.14 (d, *J* = 4.3 Hz, 2H, $H_h$), 7.96 (d, *J* = 7.8 Hz, 4H, $H_e$), 7.55 (m, 2H, $H_c$).
$^1$H NMR (500 MHz, 298 K, $CDCl_3$): δ (ppm) 8.94 (s, 2H, $H_a$), 8.80 (d, *J* = 5.0 Hz, 2H, $H_i$), 8.63 (d, *J* = 4.5 Hz, 2H, $H_b$), 8.34 (d, *J* = 8.0 Hz, 4H, $H_f$), 7.97–7.95 (m, 4H, $H_g$ & $H_d$), 7.76 (d, *J* = 8.0 Hz, 4H, $H_e$), 7.67 (d, *J* = 5.5 Hz, 2H, $H_h$),7.55 (dd, *J* = 7.5, 5.0 Hz, 2H, $H_c$).
$^{13}$C NMR (125 MHz, 298 K, $CDCl_3$): δ (ppm) 157.5, 150.9, 148.9, 148.4, 147.9, 146.4, 139.0, 138.9, 136.2, 134.4, 128.0, 127.7, 123.8, 121.8, 117.0.

HRMS (ESI, $CHCl_3/CH_3OH$): Calc. 463.192, found 463.194 for $[M+H]^+$.

**Synthesis and characterization of ligands L1, L3 and L4 in DMSO-*d*$_6$**

Ligands **L1**, **L3** and **L4** were prepared by following a modified literature procedure.[1,3]

General procedure for the synthesis of ligands **L1**, **L3**, **L4**:

In an ice-cooled ethanolic solution (60 mL) of 2-pyridinecarboxaldehyde/3-pyridinecarboxaldehyde/4-pyridinecarboxaldehyde (10 mmol) and KOH (20 mmol), 3-acetylpyridine (20 mmol) was added dropwise with vigorous stirring in a 250 mL round bottom flask. After 2 hours, 25 mL of aqueous ammonia was added, and the reaction mixture was stirred for another 12 hours at room temperature. The addition of excess water resulted in the precipitation of the product. The collected precipitate was washed with water and cold ethanol. The obtained solid was subjected to flash column chromatography if required.

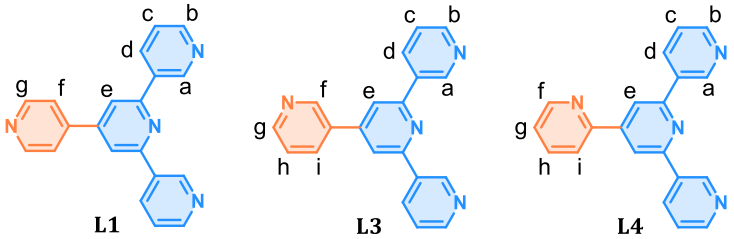


**L1**: $^1$H NMR (400 MHz, 298 K, DMSO-*d*$_6$): δ (ppm) 9.54 (s, 2H, H$_a$), 8.80 (d, *J* = 6.1 Hz, 2H, H$_g$), 8.74–8.70 (m, 4H, H$_b$ & H$_d$), 8.50 (s, 2H, H$_e$), 8.14 (d, *J* = 6.2 Hz, 2H, H$_f$), 7.60 (dd, *J* = 7.8, 4.9 Hz, 2H, H$_c$).

**L3**: $^1$H NMR (400 MHz, 298 K, DMSO-*d*$_6$): δ (ppm) 9.54 (s, 2H, H$_a$), 9.32 (s, 1H, H$_f$), 8.74–8.70 (m, 5H, H$_g$, H$_b$ & H$_d$), 8.52 (d, *J* = 8.1 Hz, 1H, H$_i$), 8.48 (s, 2H, H$_e$), 7.64–7.58 (m, 3H, H$_c$ & H$_h$).

**L4**: $^1$H NMR (400 MHz, 298 K, DMSO-*d*$_6$): δ (ppm) 9.50 (s, 2H, H$_a$), 8.83 (d, *J* = 4.6 Hz, 1H, H$_f$), 8.71–8.68 (m, 6H, H$_b$, H$_d$ & H$_e$), 8.47 (d, *J* = 7.9 Hz, 1H, H$_i$), 8.06 (dd, *J* = 7.8, 7.8 Hz, 1H, H$_h$), 7.60 (dd, *J* = 8.0, 4.8 Hz, 2H, H$_c$), 7.56 (dd, *J* = 7.5, 4.8 Hz, 1H, H$_g$).

**Synthesis of ligand L6**

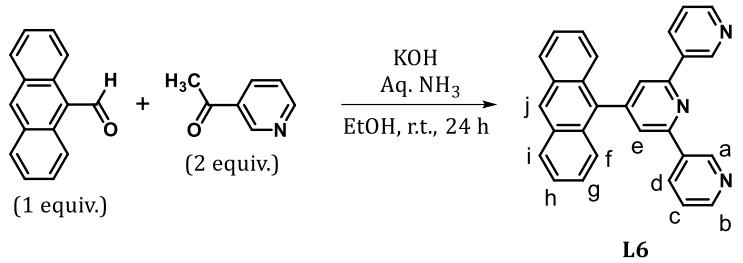


**Scheme S2** Synthesis of ligand **L6**

In a round bottom flask, 9-anthracenecarboxaldehyde (1.03 g, 5 mmol) and KOH (0.66 g, 10 mmol) were dispersed in 30 mL of ethanol. To this stirred solution, 3-acetylpyridine (1.1 mL, 10 mmol) was added dropwise and stirred for an hour. Then, 15 mL of aqueous ammonia was added, and the reaction mixture was heated at 55 °C for another 12 hours. The resultant precipitate was collected and washed several times with water, followed by cold ethanol. The product was obtained as a lime green solid (0.84 g, 42%).

**L6**: $^{1}$H NMR (400 MHz, 298 K, DMSO-$d_6$): δ (ppm) 9.52 (s, 2H, $H_a$), 8.80 (s, 1H, $H_j$), 8.72–8.68 (m, 4H, $H_b$ & $H_d$), 8.24 (s, 2H, $H_e$), 8.22 (d, $J$ = 8.5 Hz, 2H, $H_f$), 7.67 (d, $J$ = 8.8 Hz, 2H, $H_i$), 7.60–7.54 (m, 4H, $H_c$ & $H_g$), 7.49 (dd, 2H, $H_h$).

$^{1}$H NMR (400 MHz, 298 K, $CDCl_3$): δ (ppm) 9.42 (s, 2H, $H_a$), 8.70 (d, $J$ = 4.6 Hz, 2H, $H_b$), 8.60 (s, 1H, $H_j$), 8.54 (d, $J$ = 8.0 Hz, 2H, $H_d$), 8.10 (d, $J$ = 8.4 Hz, 2H, $H_f$), 7.91 (s, 2H, $H_e$), 7.69 (d, $J$ = 8.8 Hz, 2H, $H_i$), 7.53–7.41 (m, 6H, $H_c$, $H_g$ & $H_h$).

$^{13}$C NMR (100 MHz, 298 K, $CDCl_3$): δ (ppm) 155.2, 150.4, 150.0, 148.7, 134.7, 134.5, 133.4, 131.4, 129.6, 128.8, 128.1, 126.5, 125.8, 125.6, 123.8, 122.3.

HRMS (ESI, $CHCl_3$/$CH_3OH$): Calc. 410.165, found 410.165 for $[M+H]^+$.

**Stoichiometry controlled synthesis of 1a**

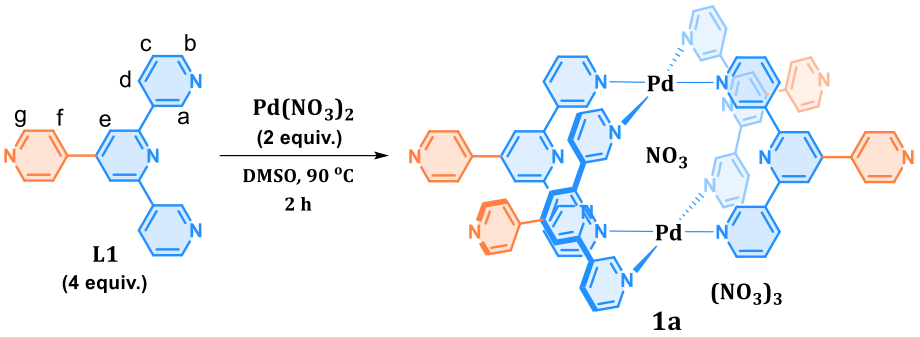


**Scheme S3** Stoichiometry controlled synthesis of $(NO_3)\subset$**1**$\cdot 3NO_3$, **1a**.

In an NMR tube, 40 μL DMSO-$d_6$ solution of $Pd(NO_3)_2\cdot 2H_2O$ (0.53 mg, 50 mM) and ligand **L1** (1.24 mg) were mixed in an additional 360 μL of DMSO-$d_6$ to prepare 2.5 mM of $(NO_3)\subset$**1**$\cdot 3NO_3$, **1a**. The reaction mixture was heated at 90 °C for 2 h. $^1$H NMR spectral analysis showed the presence of a discrete assembly comparable to that of the nitrate-encapsulated $Pd_2L_4$ cage reported earlier in Chapter 2. The 3,2':6',3''-terpyridine proton signals suffered a significant downfield shift, while outer 4-pyridyl proton signals were slightly upfield shifted. This indicates that only 3,2':6',3''-terpyridine unit complexed with Pd(II).

$^1$H NMR (500 MHz, 298 K, DMSO-$d_6$): δ (ppm) 11.29 (s, 8H, $H_a$), 9.76 (d, $J$ = 5.5 Hz, 8H, $H_b$), 9.04 (d, $J$ = 8.1 Hz, 8H, $H_d$), 8.74 (d, $J$ = 4.3 Hz, 8H, $H_g$), 8.54 (s, 8H, $H_e$), 8.03–7.97 (m, 16H, $H_c$ & $H_f$).

HRMS (ESI, DMSO) ($m/z$): Calc. for [**1a**–$NO_3$]$^{1+}$ 1640.262, found 1640.254; Calc. for [**1a**–$2NO_3$]$^{2+}$ 789.137, found 789.133; Calc. for [**1a**–$3NO_3$]$^{3+}$ 505.429, found 505.425.

**Stoichiometry controlled synthesis of 2a**

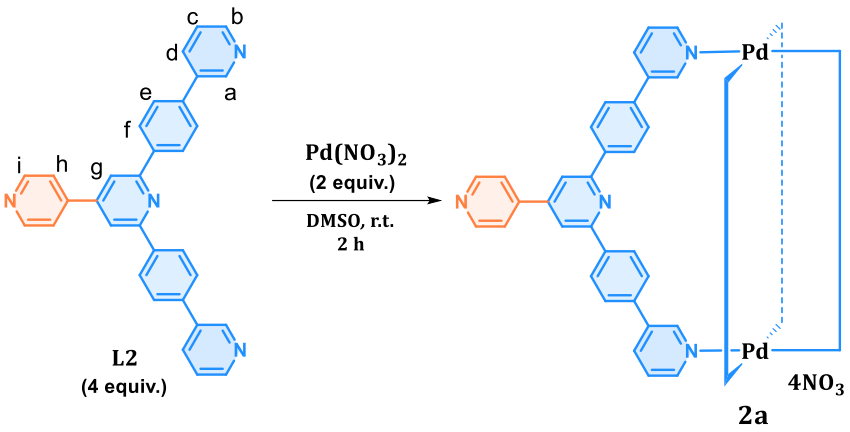


**Scheme S4** Stoichiometry controlled synthesis of **2**·4$NO_3$, **2a**.

In an NMR tube, 40 μL DMSO-$d_6$ solution of $Pd(NO_3)_2 \cdot 2H_2O$ (0.53 mg, 50 mM) and ligand **L2** (1.85 mg) were mixed in an additional 360 μL of DMSO-$d_6$ to prepare 2.5 mM of **2**·4$NO_3$, **2a**. The reaction mixture was stirred at room temperature for 2 h. The $^1$H NMR spectral analysis showed the presence of a discrete assembly.

$^1$H NMR (400 MHz, 298 K, DMSO-$d_6$): δ (ppm) 10.01 (s, $H_a$), 9.63 (d, $J$ = 5.6 Hz, $H_b$), 8.75 (d, $J$ = 4.8 Hz, $H_i$), 8.71 (d, $J$ = 8.0 Hz, $H_f$), 8.60 (d, $J$ = 8.5 Hz, $H_d$), 8.41 (s, $H_g$), 8.20 (d, $J$ = 7.8 Hz, $H_e$), 8.07 (d, $J$ = 4.8 Hz, $H_h$), 7.95 (dd, $H_c$).

HRMS (ESI, DMSO) (*m/z*): Calc. for [**2a**–2$NO_3$]$^{2+}$ 1093.263, found 1093.257; Calc. for [**2a**–3$NO_3$]$^{3+}$ 708.180, found 708.175; Calc. for [**2a**–4$NO_3$]$^{4+}$ 515.638, found 515.633.

**Stoichiometry controlled synthesis of 3a**

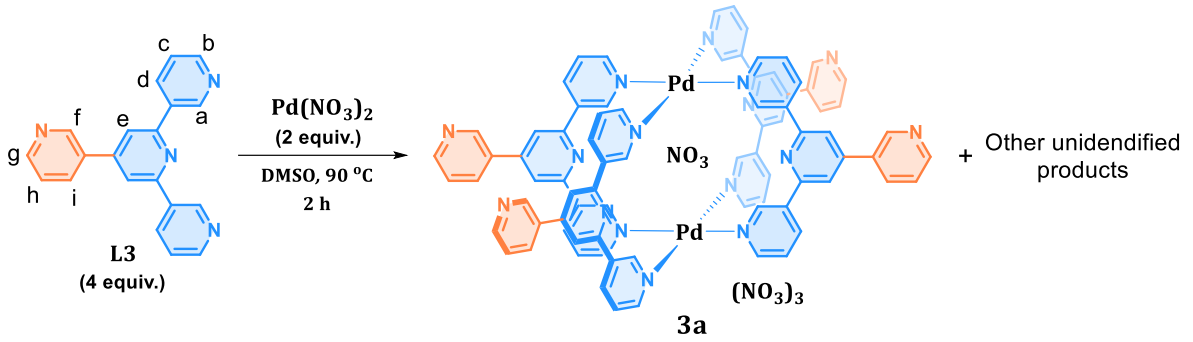


**Scheme S5** Stoichiometry controlled synthesis of $(NO_3)\subset$**3**$\cdot 3NO_3$, **3a**.

In an NMR tube, 40 μL DMSO-$d_6$ solution of $Pd(NO_3)_2\cdot 2H_2O$ (0.53 mg, 50 mM) and ligand **L3** (1.24 mg) were mixed with an additional 360 μL of DMSO-$d_6$ to prepare 2.5 mM of $(NO_3)\subset$**3**$\cdot 3NO_3$, **3a**. The reaction mixture was heated at 90 °C for 2 h. $^1$H NMR spectral analysis showed the presence of a mixture of assemblies in contrast to the synthesis of $(NO_3)\subset$**1**$\cdot 3NO_3$.

HRMS (ESI, DMSO) (*m/z*): Calc. for [**3a**–$NO_3$]$^{1+}$ 1640.262, found 1640.240; Calc. for [**3a**–$2NO_3$]$^{2+}$ 789.137, found 789.117; Calc. for [**3a**–$3NO_3$]$^{3+}$ 505.429, found 505.417.

**Stoichiometry controlled synthesis of 4a**

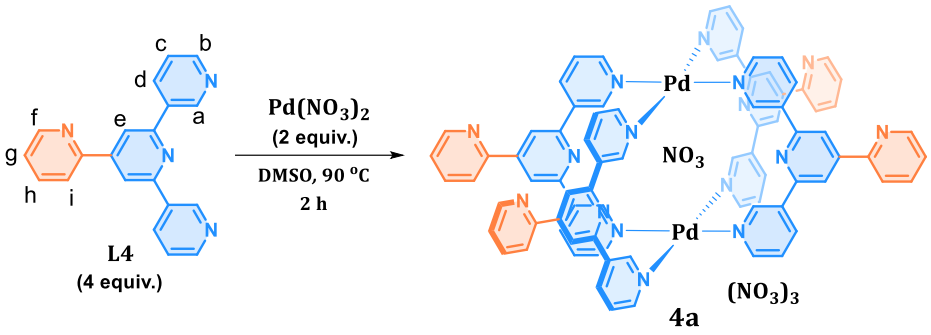


**Scheme S6** Stoichiometry controlled synthesis of $(NO_3)\subset$**4**$\cdot 3NO_3$, **4a**.

In an NMR tube, 40 μL DMSO-$d_6$ solution of $Pd(NO_3)_2\cdot 2H_2O$ (0.53 mg, 50 mM) and ligand **L4** (1.24 mg) were mixed with an additional 360 μL of DMSO-$d_6$ to prepare 2.5 mM of $(NO_3)\subset$**4**$\cdot 3NO_3$, **4a**. The reaction mixture was heated at 90 °C for 2 h. $^1$H NMR spectral analysis showed the presence of a discrete assembly comparable to that of the nitrate-encapsulated $Pd_2L_4$ cage, **1a**. The 3,2':6',3''-terpyridine proton signals suffered a significant downfield shift, while outer 4-pyridyl proton signals were slightly upfield shifted. This indicates that only 3,2':6',3''-terpyridine unit complexed with Pd(II).

$^1$H NMR (400 MHz, 298 K, DMSO-$d_6$): δ (ppm) 11.31 (s, 8H, $H_a$), 9.76 (d, J = 5.7 Hz, 8H, $H_b$), 8.98 (d, J = 8.2 Hz, 8H, $H_d$), 8.73 (m, 12H, $H_e$ & $H_f$), 8.31 (d, J = 8.0 Hz, 4H, $H_i$), 8.02–7.96 (m, 12H, $H_c$ & $H_h$), 7.51 (dd, J = 4.9, 7.4 Hz, 4H, $H_g$).

HRMS (ESI, DMSO) (*m/z*): Calc. for [**4a**$-2NO_3]^{2+}$ 789.137, found 789.102; Calc. for [**4a**$-3NO_3]^{3+}$ 505.429, found 505.415.

**Synthesis of $(NO_3)\subset$6·3$NO_3$, 6a**

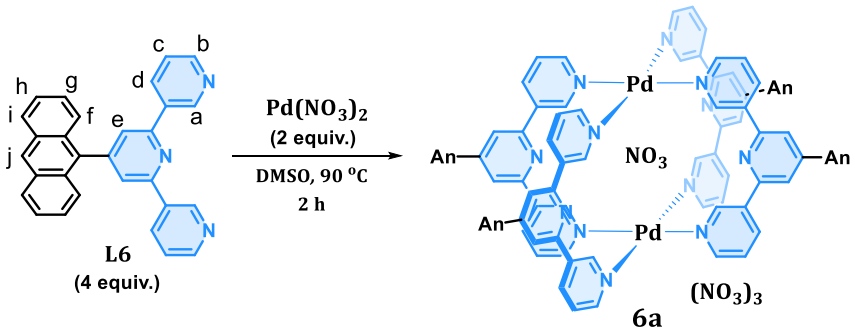


**Scheme S7** Synthesis of $(NO_3)\subset$**6**·3$NO_3$, **6a**.

In an NMR tube, 40 μL DMSO-$d_6$ solution of $Pd(NO_3)_2{\cdot}2H_2O$ (0.53 mg, 50 mM) and ligand **L6** (1.64 mg) were mixed with an additional 360 μL of DMSO-$d_6$ to prepare 2.5 mM of $(NO_3)\subset$**6**·3$NO_3$, **6a**. The reaction mixture was heated at 90 °C for 2 h. The $^1$H NMR spectral analysis showed the presence of a discrete assembly comparable to that of the nitrate-encapsulated $Pd_2L_4$ cage, **1a**. The 3,2':6',3''-terpyridine proton signals suffered a considerable downfield shift indicating the formation of nitrate-encapsulated cage, $(NO_3)\subset$**6**·3$NO_3$, **6a**.

$^1$H NMR (400 MHz, 298 K, DMSO-$d_6$): δ (ppm) 11.60 (s, 2H, $H_a$), 9.74 (d, $J$ = 5.6 Hz, 2H, $H_b$), 8.93 (d, $J$ = 8.2 Hz, 2H, $H_b$), 8.81 (s, 1H, $H_j$), 8.46 (s, 2H, $H_e$), 8.21 (d, $J$ = 8.5 Hz, 2H, $H_f$), 7.67 (dd, $J$ = 8.0, 5.9 Hz, 2H, $H_c$), 7.58–7.54 (m, 4H, $H_i$ & $H_g$), 7.39 (dd, 2H, $H_h$).

HRMS (ESI, DMSO) ($m/z$): Calc. for [**6a**–$NO_3$]$^{1+}$ 2036.407, found 2036.403; Calc. for [**6a**–2$NO_3$]$^{2+}$ 987.210, found 987.209; Calc. for [**6a**–3$NO_3$]$^{3+}$ 637.478, found 637.477.

## 3. NMR characterization data

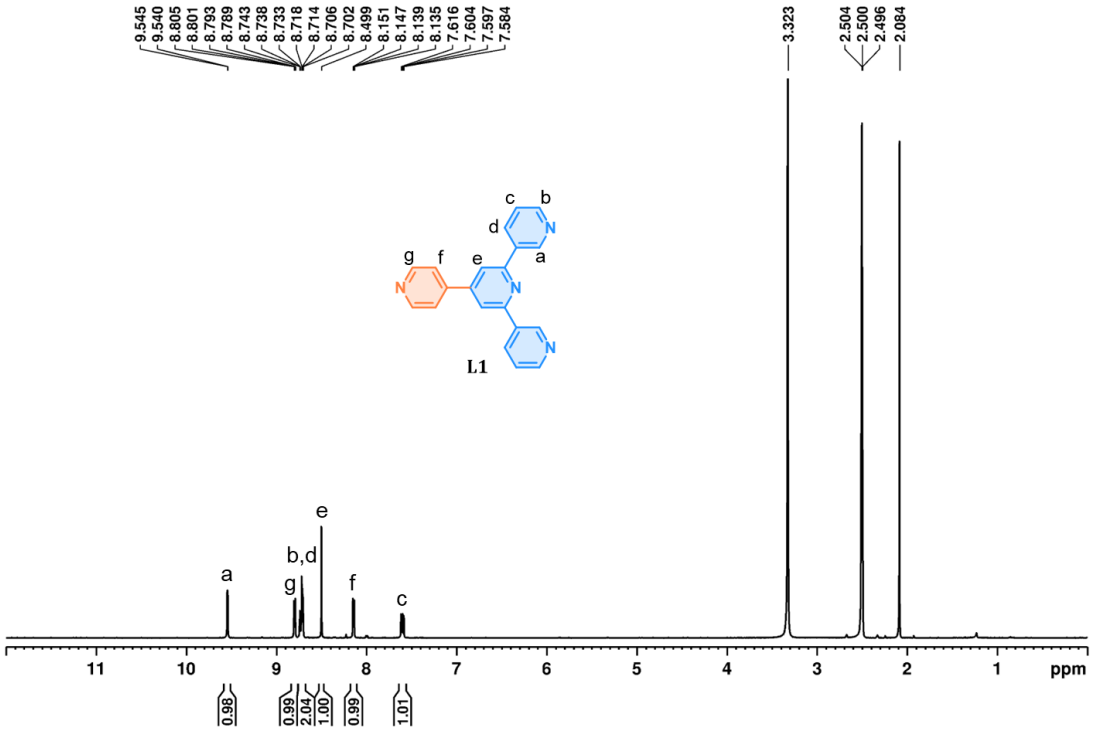


**Figure S1** $^{1}$H NMR spectrum (400 MHz, 298 K) in DMSO-$d_6$ for **L1**.

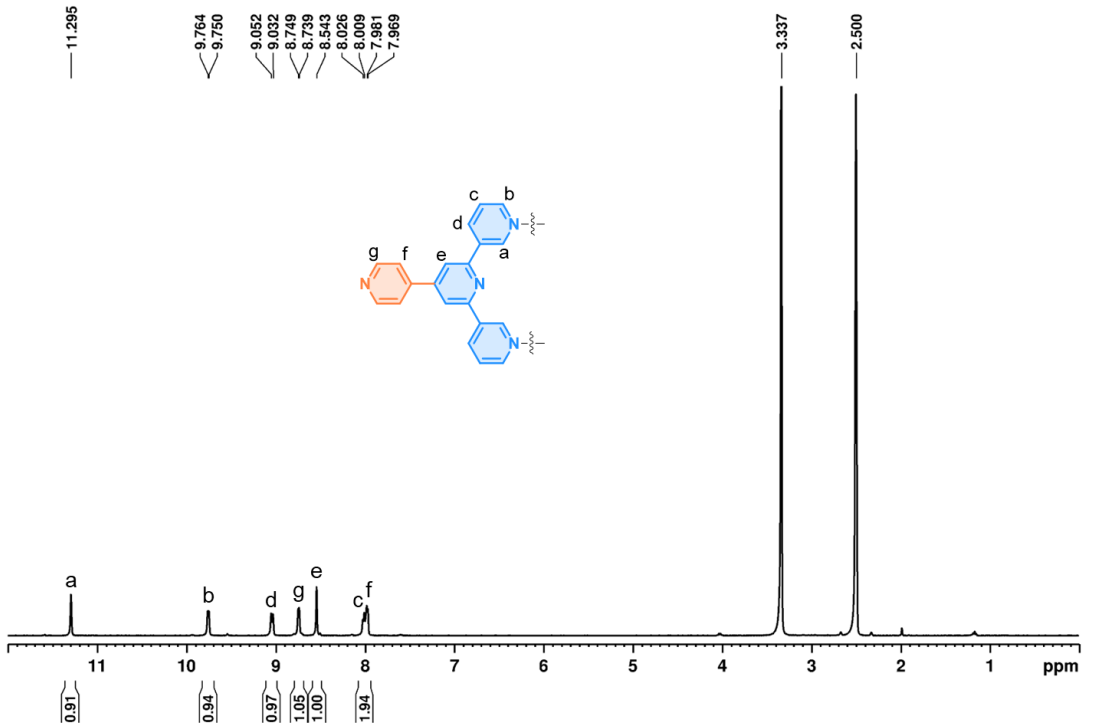


**Figure S2** $^{1}$H NMR spectrum (400 MHz, 298 K) in DMSO-$d_6$ for **1a**.

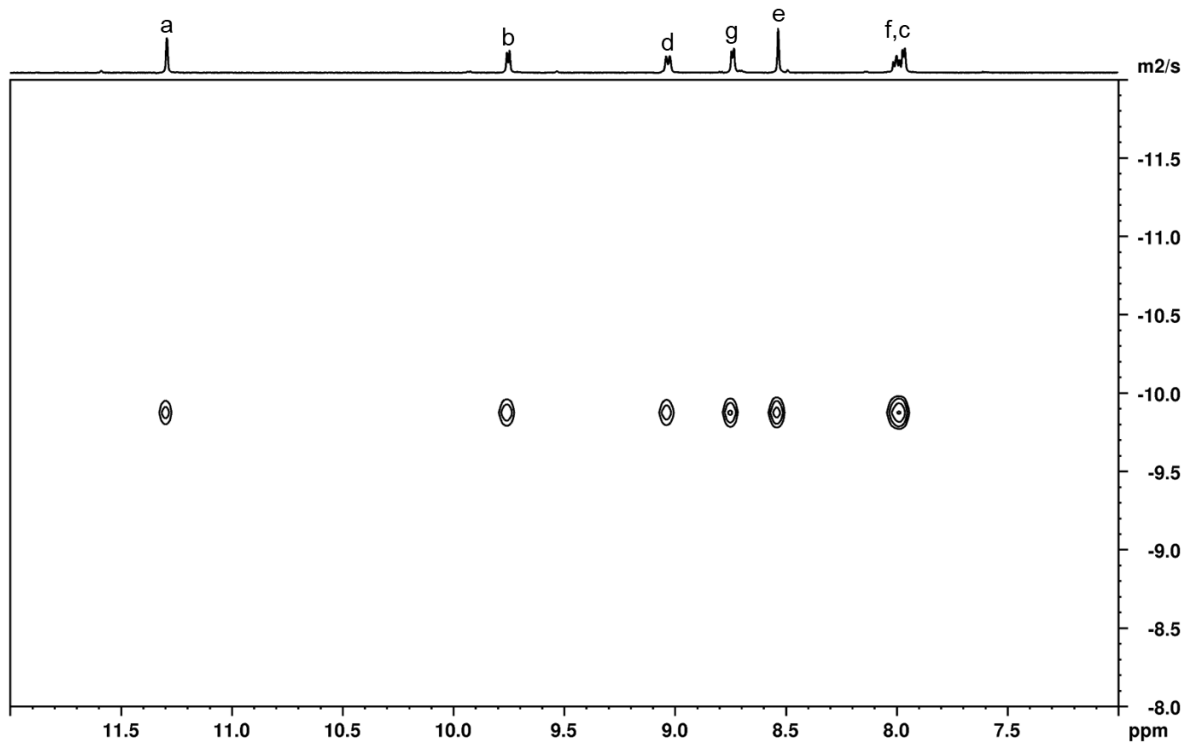


**Figure S3** $^{1}$H DOSY NMR spectrum (500 MHz, 298 K) in DMSO-$d_6$ for **$NO_3$⊂1**·3$NO_3$, **1a**. Diffusion coefficient, D = 1.33 x $10^{-10}$ $m^2$/s.

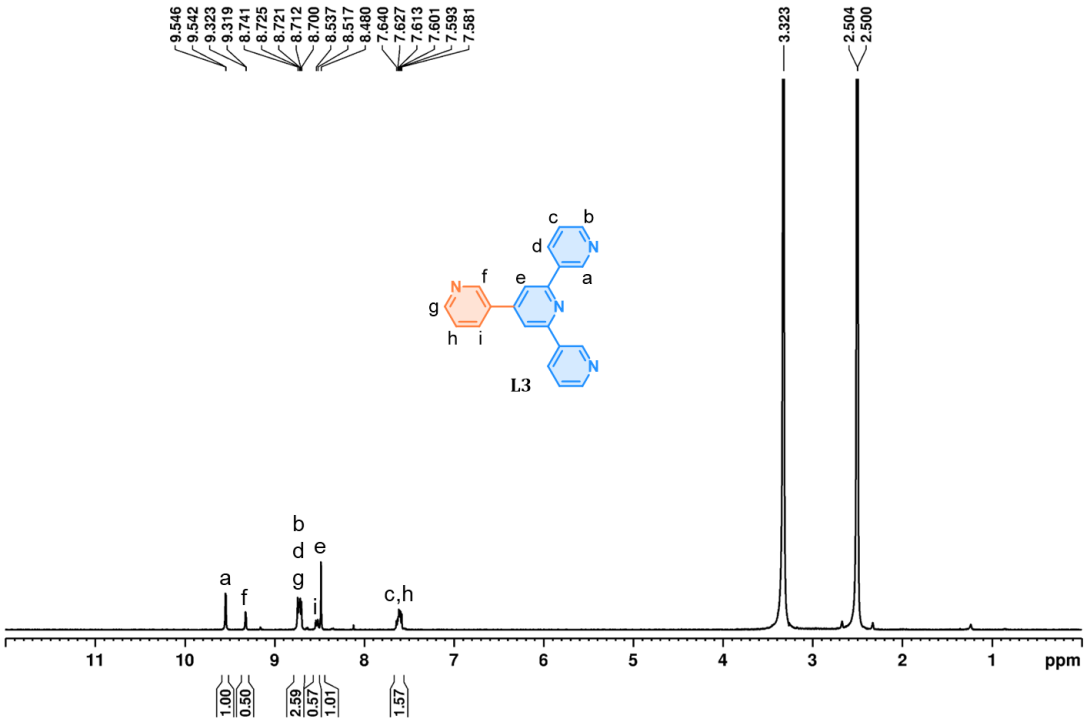


**Figure S4** $^{1}$H NMR spectrum (400 MHz, 298 K) in DMSO-$d_6$ for **L3**.

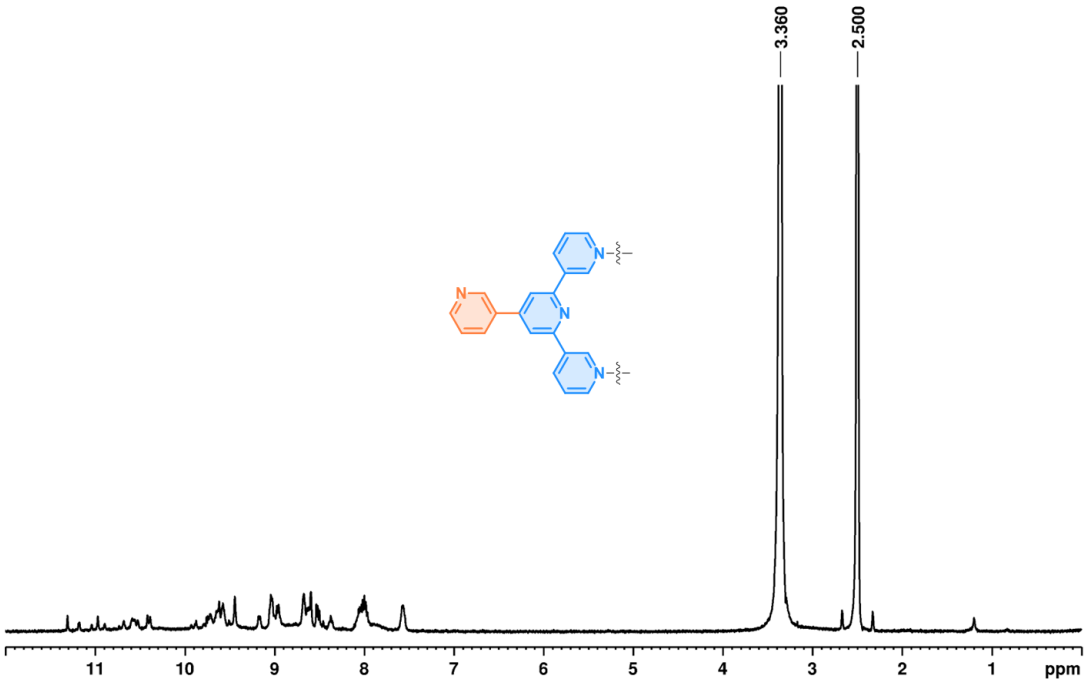


**Figure S5** $^{1}$H NMR spectrum (400 MHz, 298 K) in DMSO-$d_6$ for the addition of $Pd(NO_3)_2$ to **L3** (2:4 ratio) after 2 hours at 90 °C.

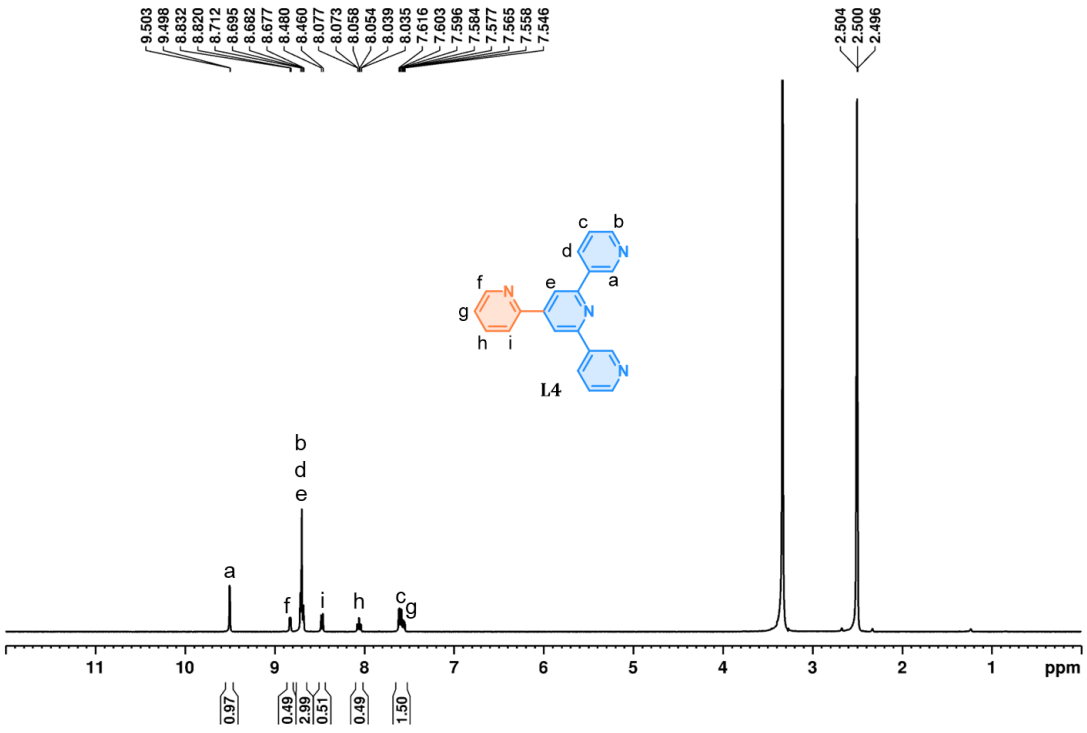


**Figure S6** $^{1}$H NMR spectrum (400 MHz, 298 K) in DMSO-$d_6$ for **L4**.

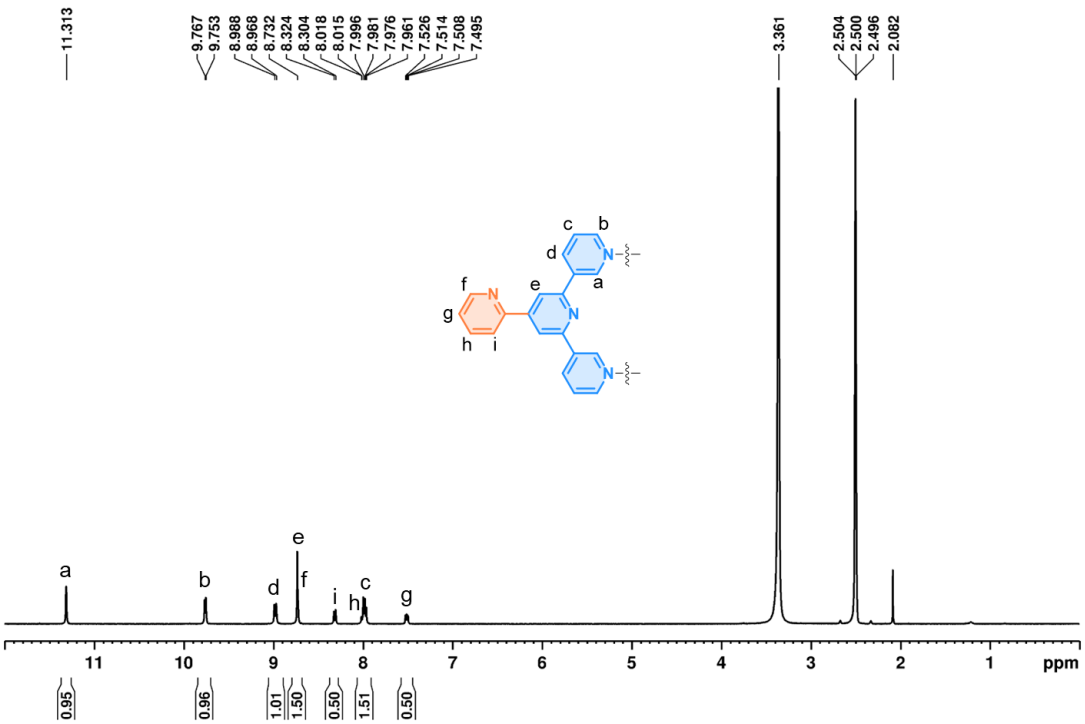


**Figure S7** $^{1}$H NMR spectrum (400 MHz, 298 K) in DMSO-$d_6$ for **4a**.

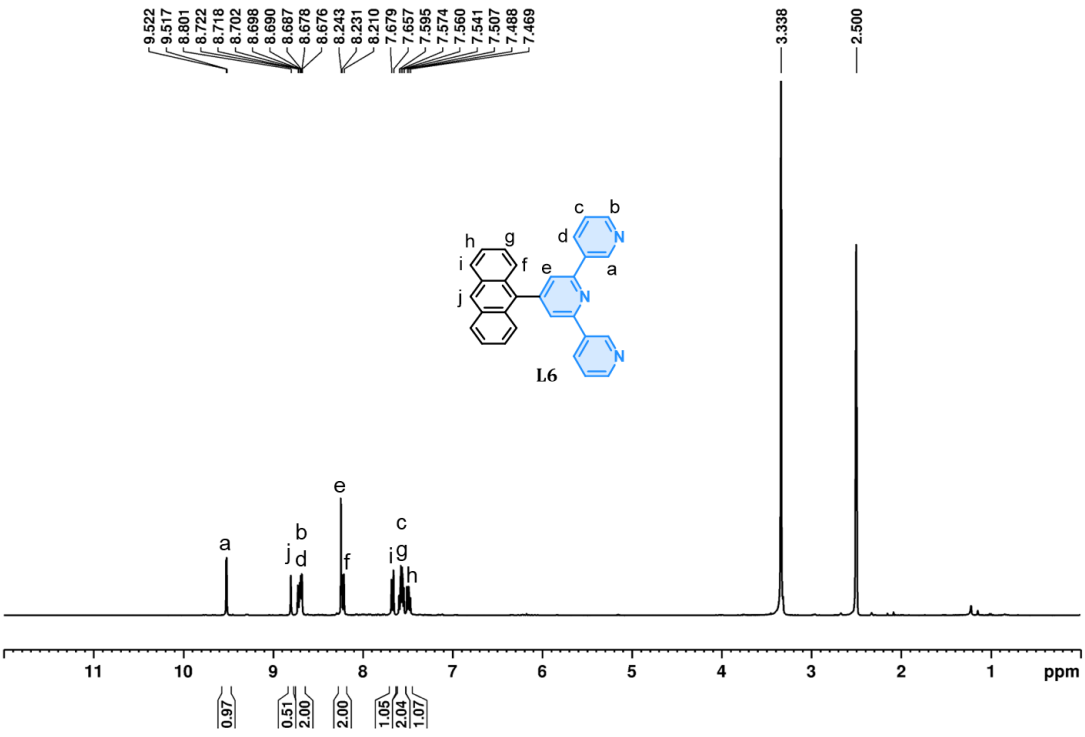


**Figure S8** $^{1}$H NMR spectrum (400 MHz, 298 K) in DMSO-$d_6$ for **L6**.

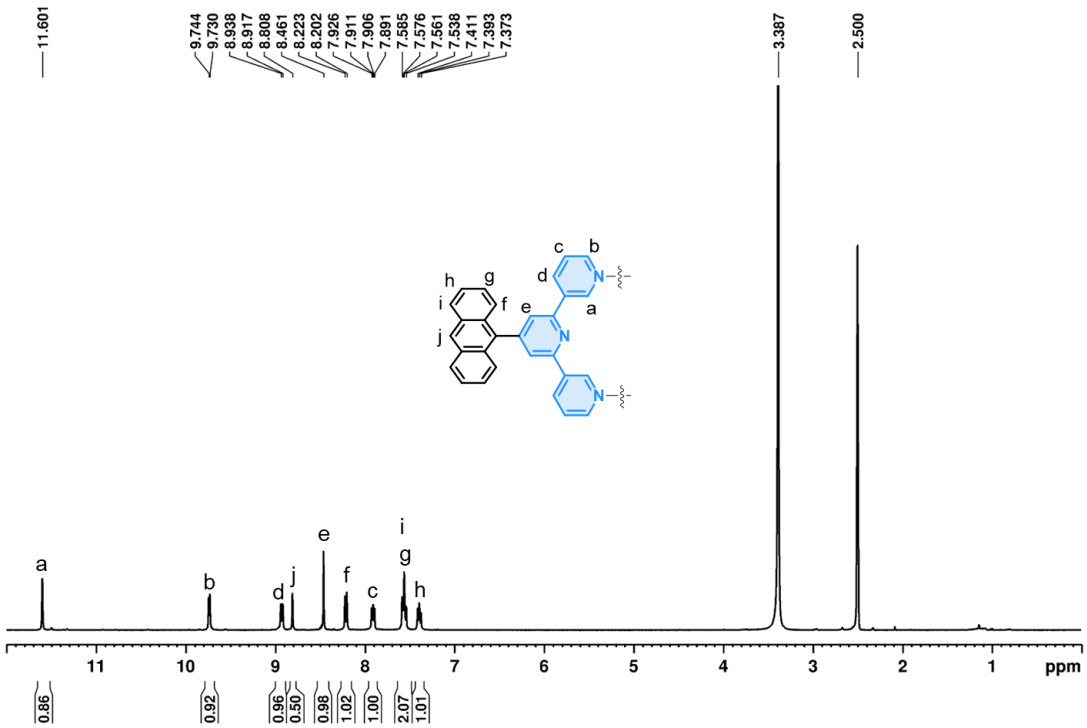


**Figure S9** $^{1}$H NMR spectrum (400 MHz, 298 K) in DMSO-$d_6$ for **6a**.

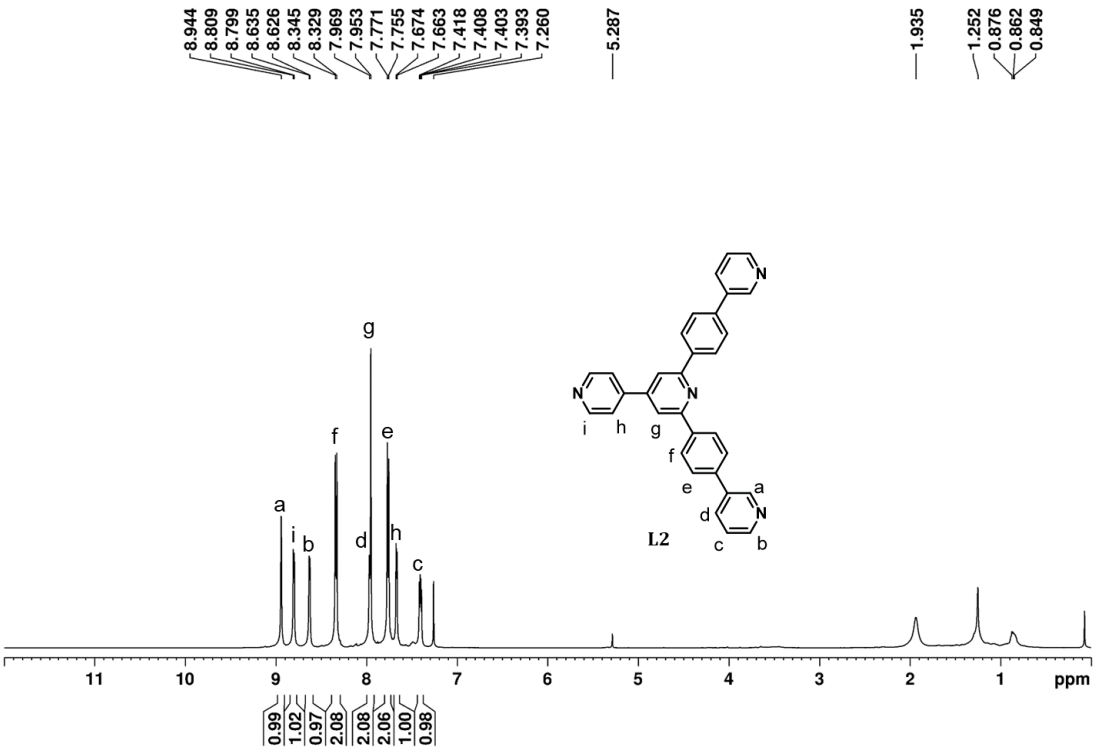


**Figure S10** $^{1}$H NMR spectrum (400 MHz, 298 K) in $CDCl_3$ for **L2**.

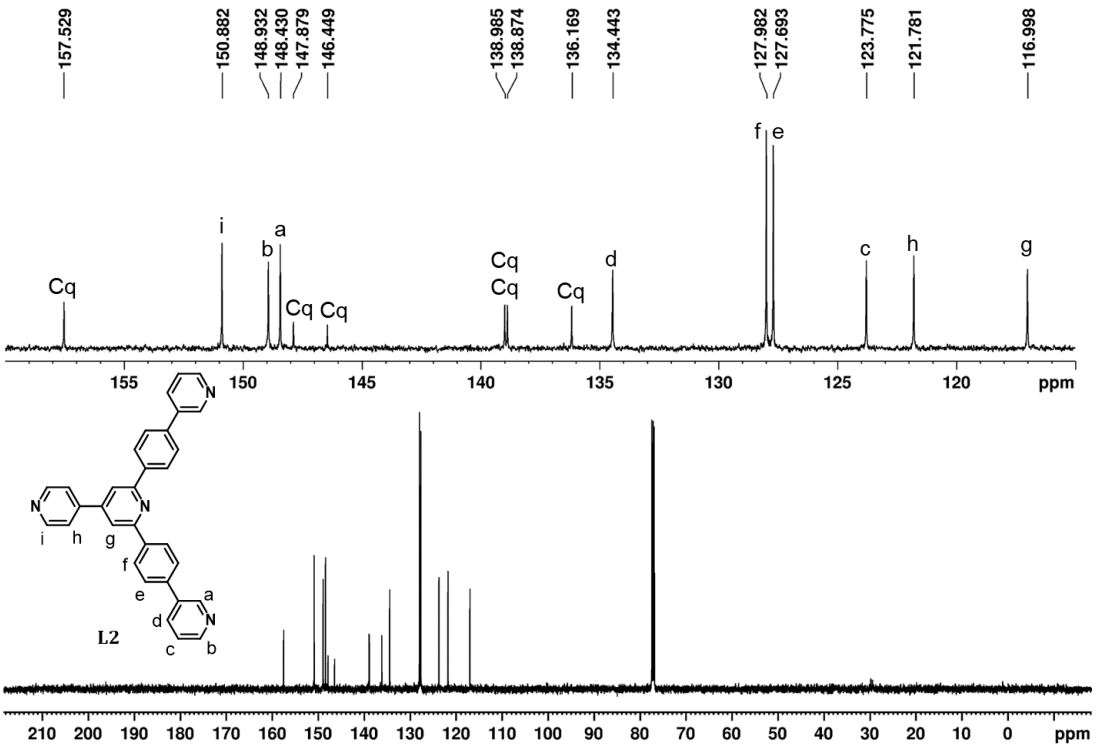


**Figure S11** $^{13}$C NMR spectrum (400 MHz, 298 K) in $CDCl_3$ for **L2**.

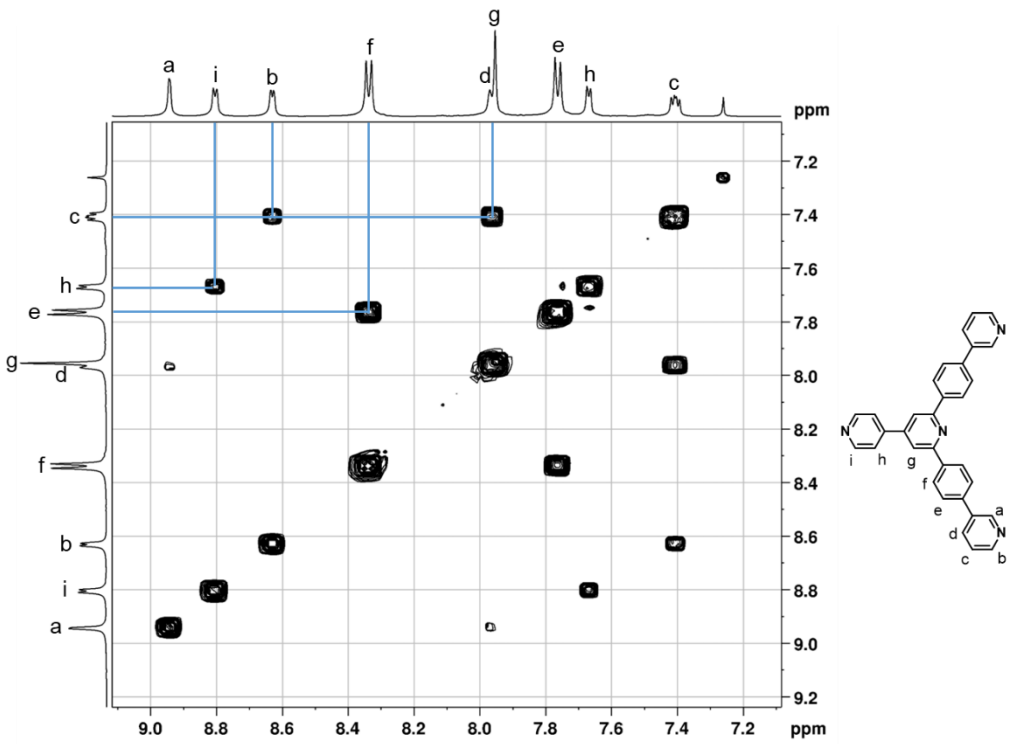


**Figure S12** $^{1}$H–$^{1}$H COSY NMR spectrum (400 MHz, 298 K) in $CDCl_3$ for **L2**.

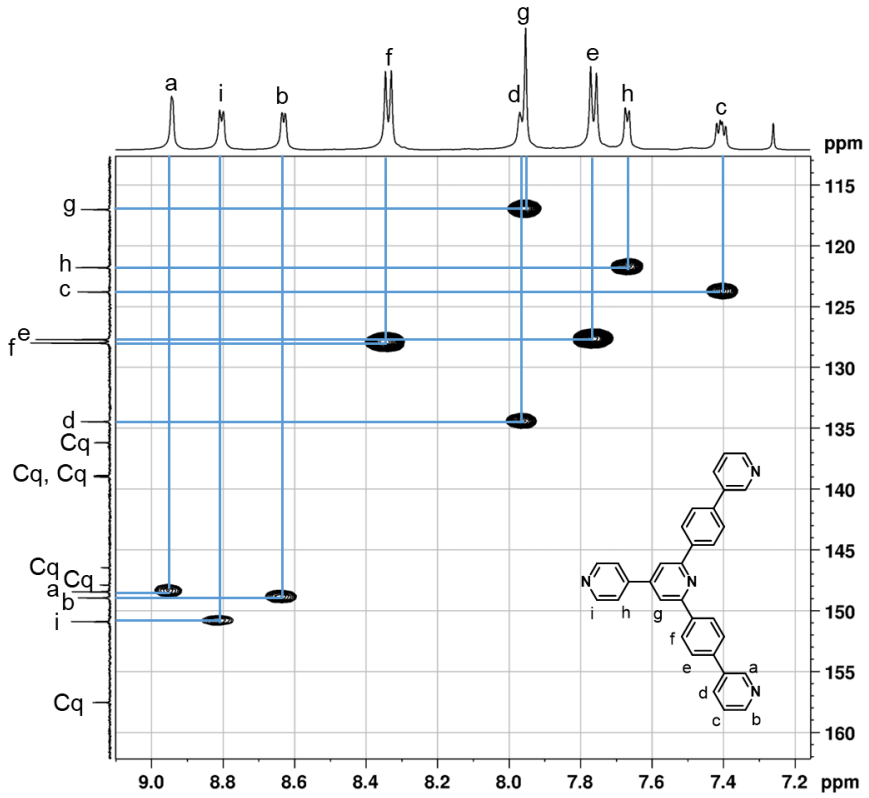


**Figure S13** $^{1}H–^{13}C$ HSQC NMR spectrum (400 MHz, 298 K) in $CDCl_3$ for **L2**.

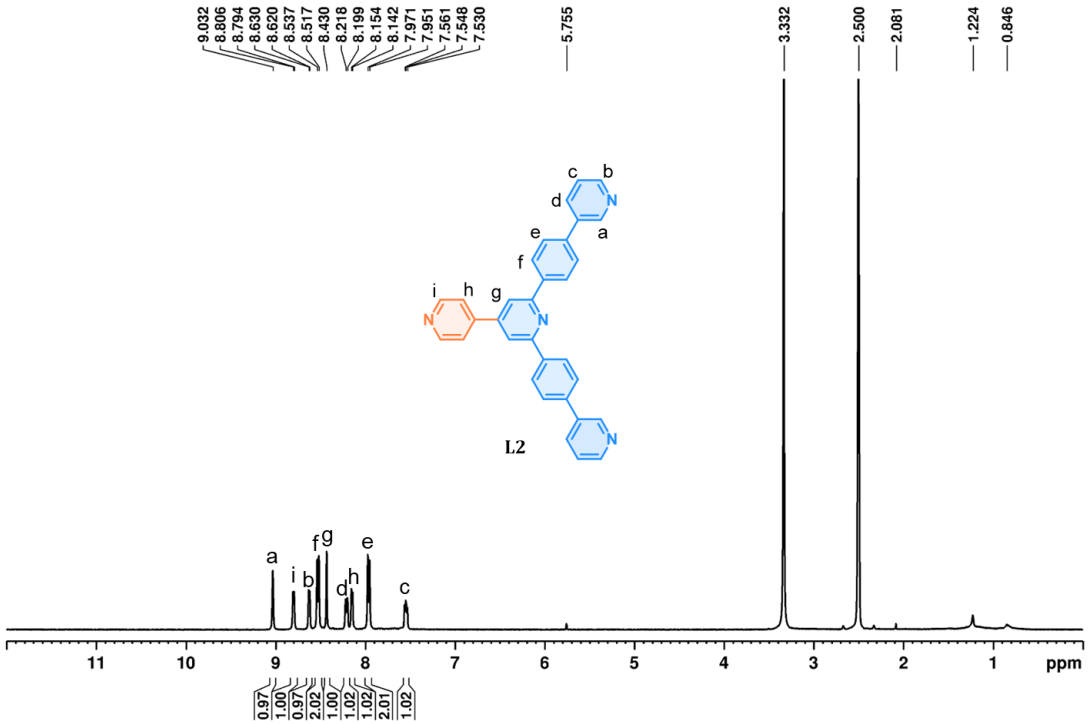


**Figure S14** $^{1}H$ NMR spectrum (400 MHz, 298 K) in DMSO-$d_6$ for **L2**.

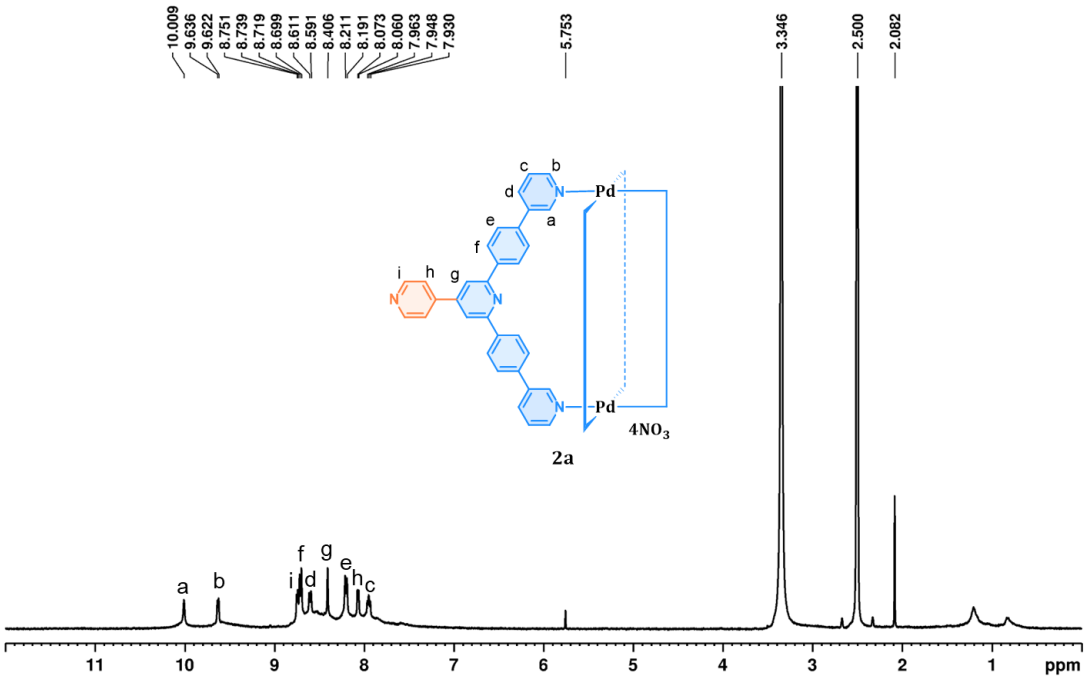


**Figure S15** $^{1}$H NMR spectrum (400 MHz, 298 K) in DMSO-$d_6$ for **2a**.

## 4. Mass spectrometry data

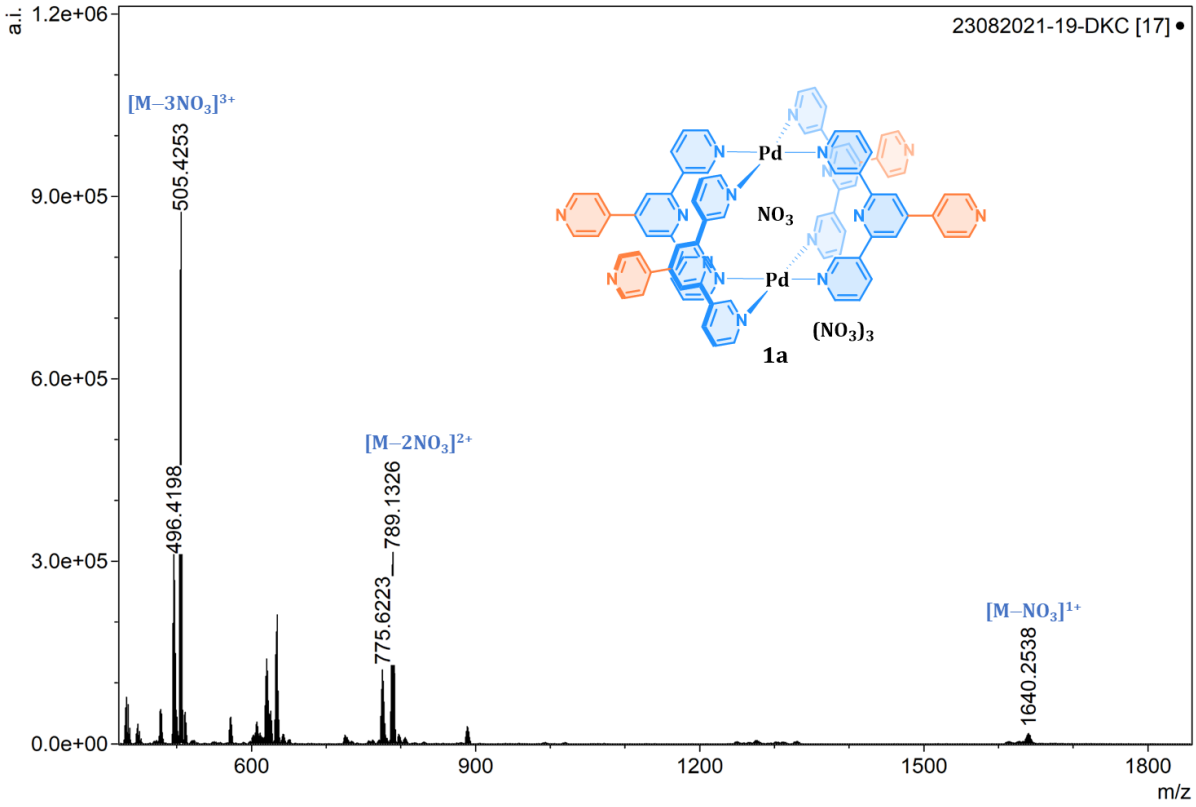


**Figure S16** ESI mass spectral analysis of **NO$_3$⊂1**·3NO$_3$.

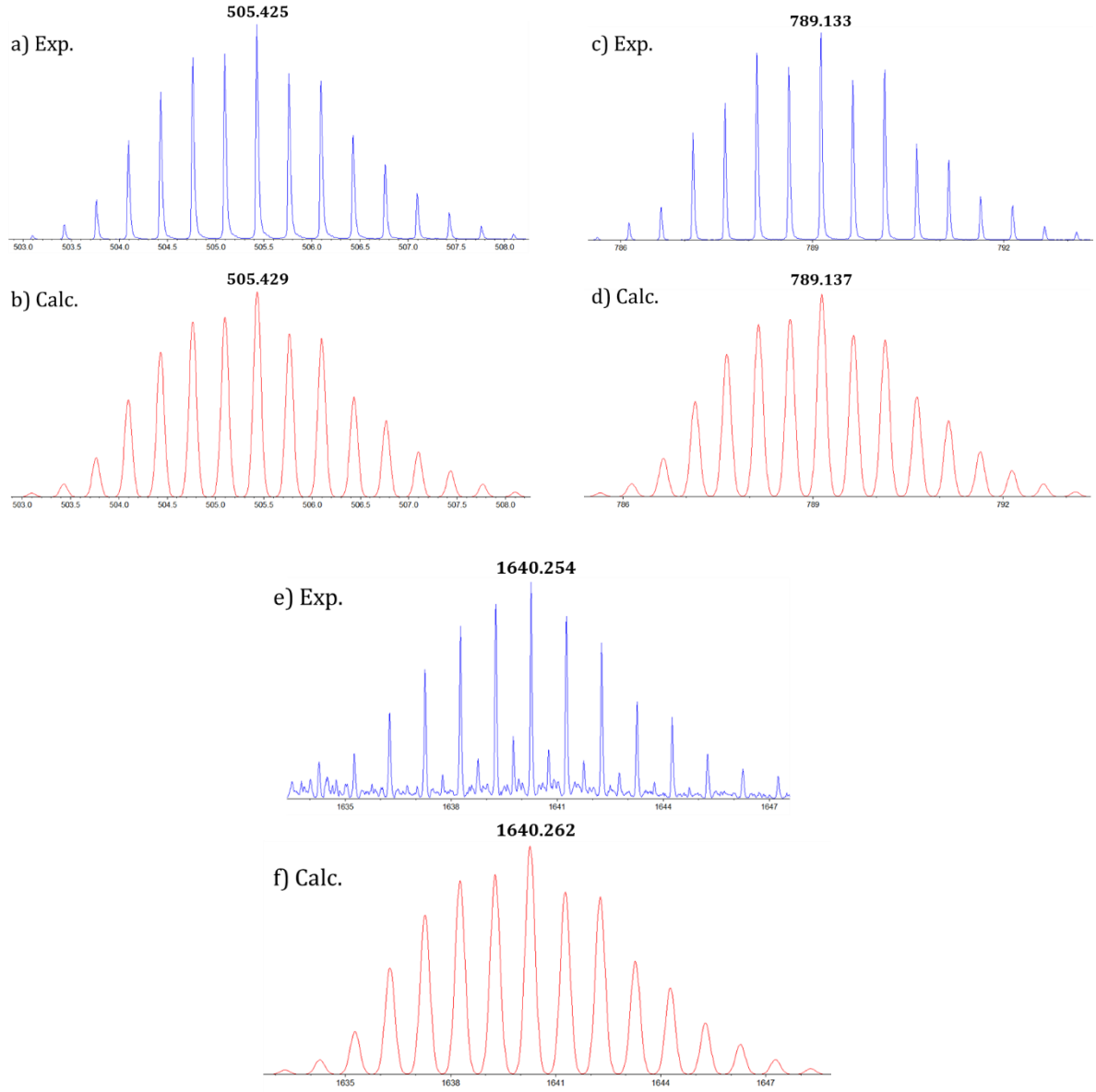


**Figure S17** Experimental (a, c & e) and theoretical (b, d & f) isotopic pattern for [**1a**–3$NO_3$]$^{3+}$, [**1a**–2$NO_3$]$^{2+}$ and [**1a**–$NO_3$]$^{1+}$ respectively.

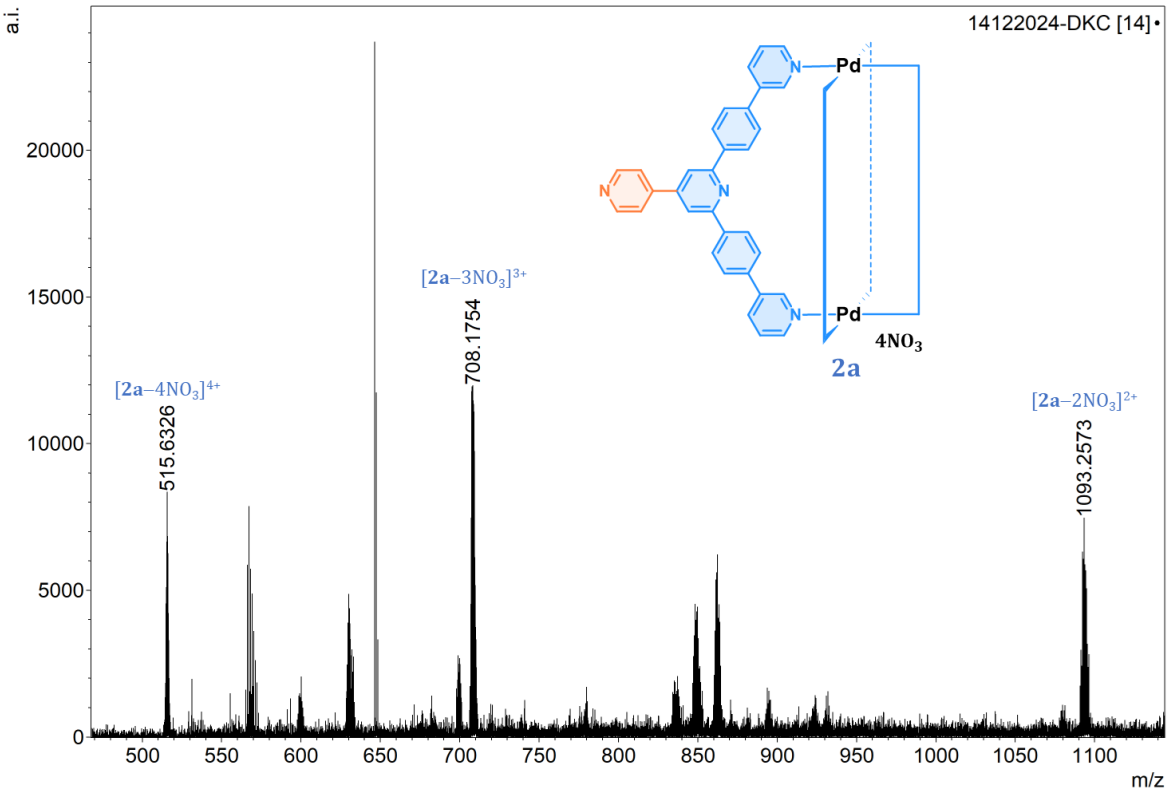


**Figure S18** ESI mass spectral analysis of **2**·4$NO_3$, **2a**.

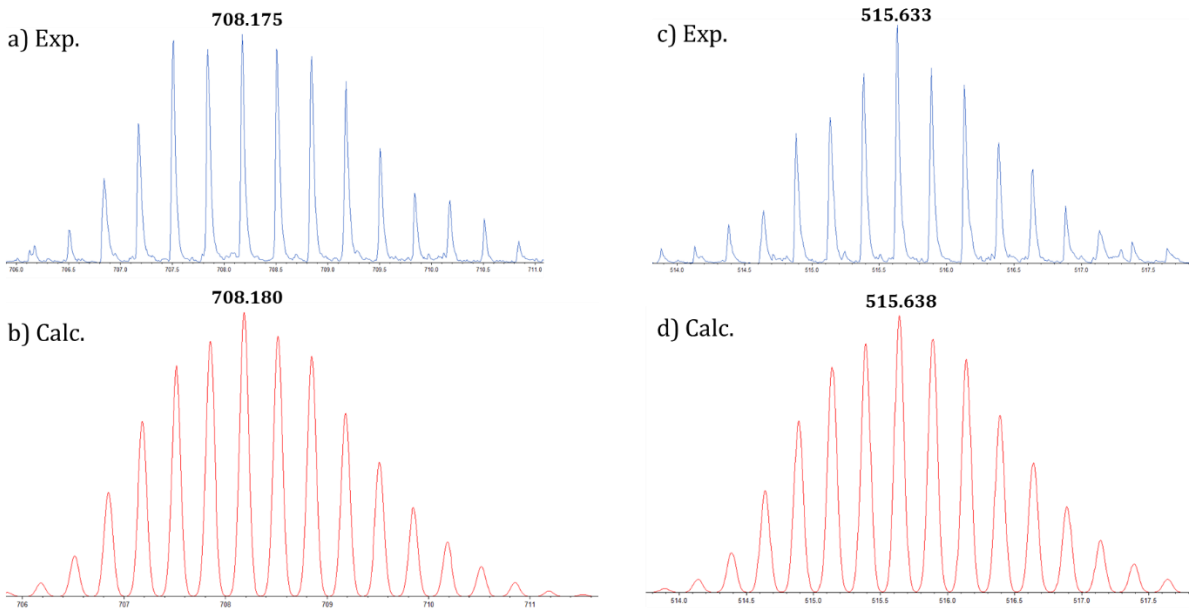


**Figure S19** Experimental (a & c) and theoretical (b & d) isotopic pattern for [**2a**–3$NO_3$]$^{3+}$ and [**2a**–4$NO_3$]$^{4+}$ respectively.

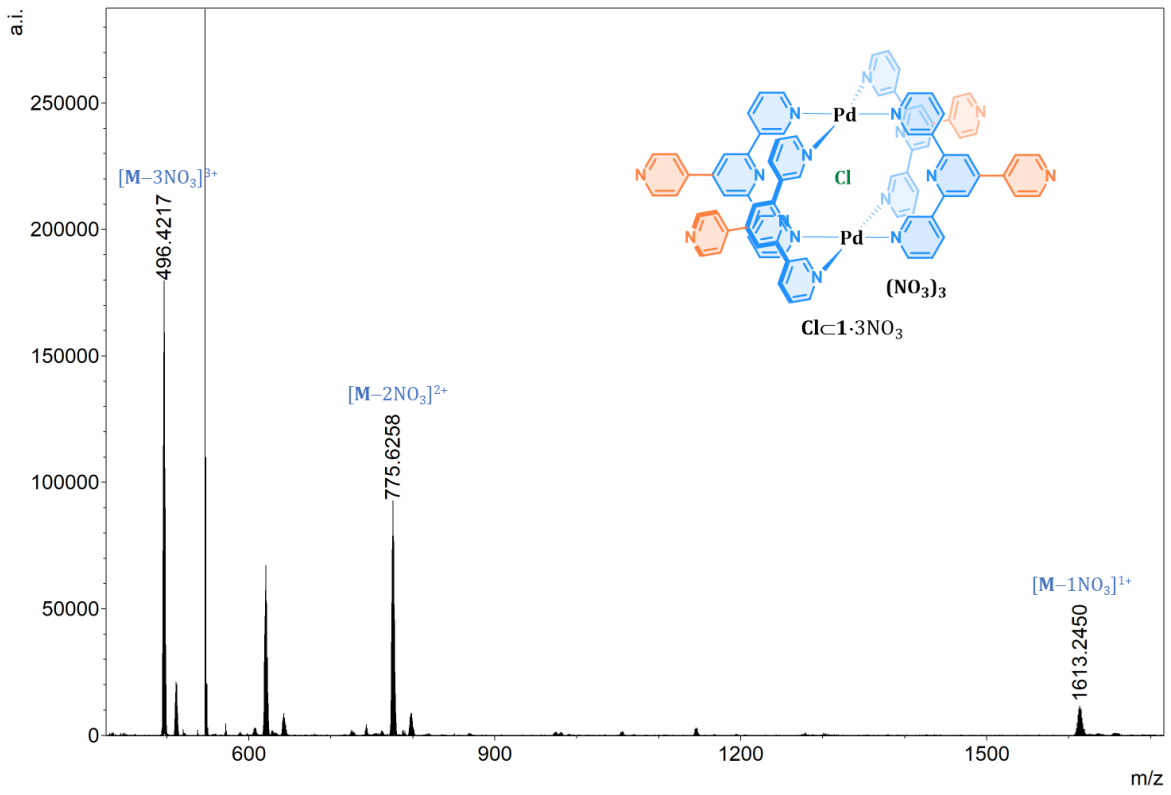


**Figure S20** ESI mass spectral analysis of **Cl⊂1**·3$NO_3$.

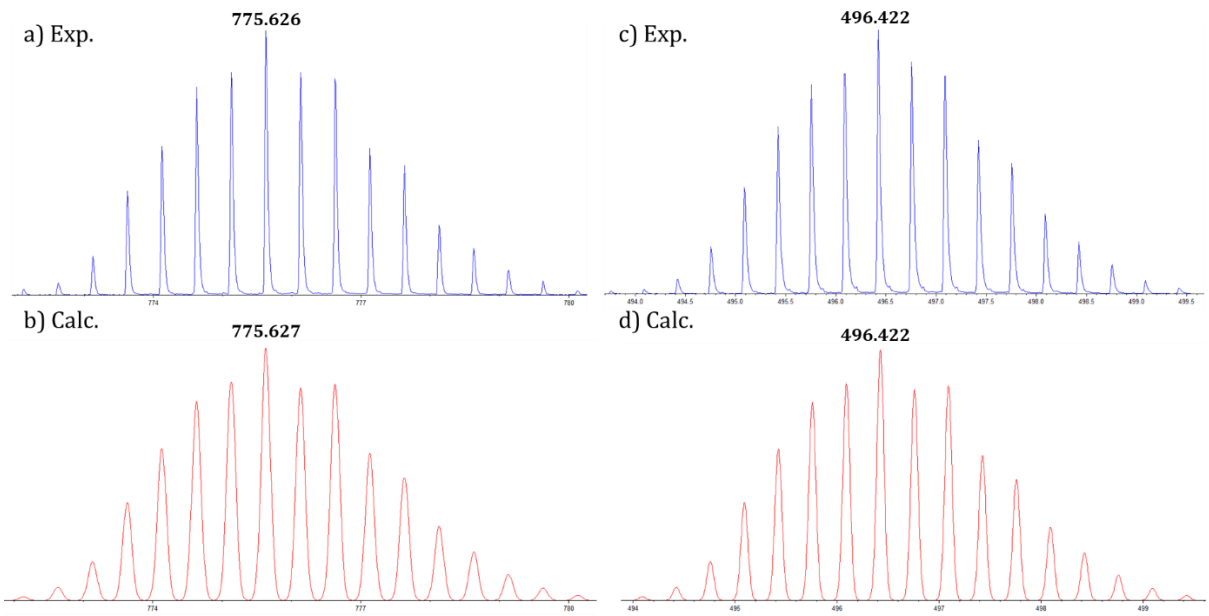


**Figure S21** Experimental (a & c) and theoretical (b & d) isotopic pattern for [**Cl⊂1**·3$NO_3$–2$NO_3$]$^{2+}$ and [**Cl⊂1**·3$NO_3$–3$NO_3$]$^{3+}$ respectively.

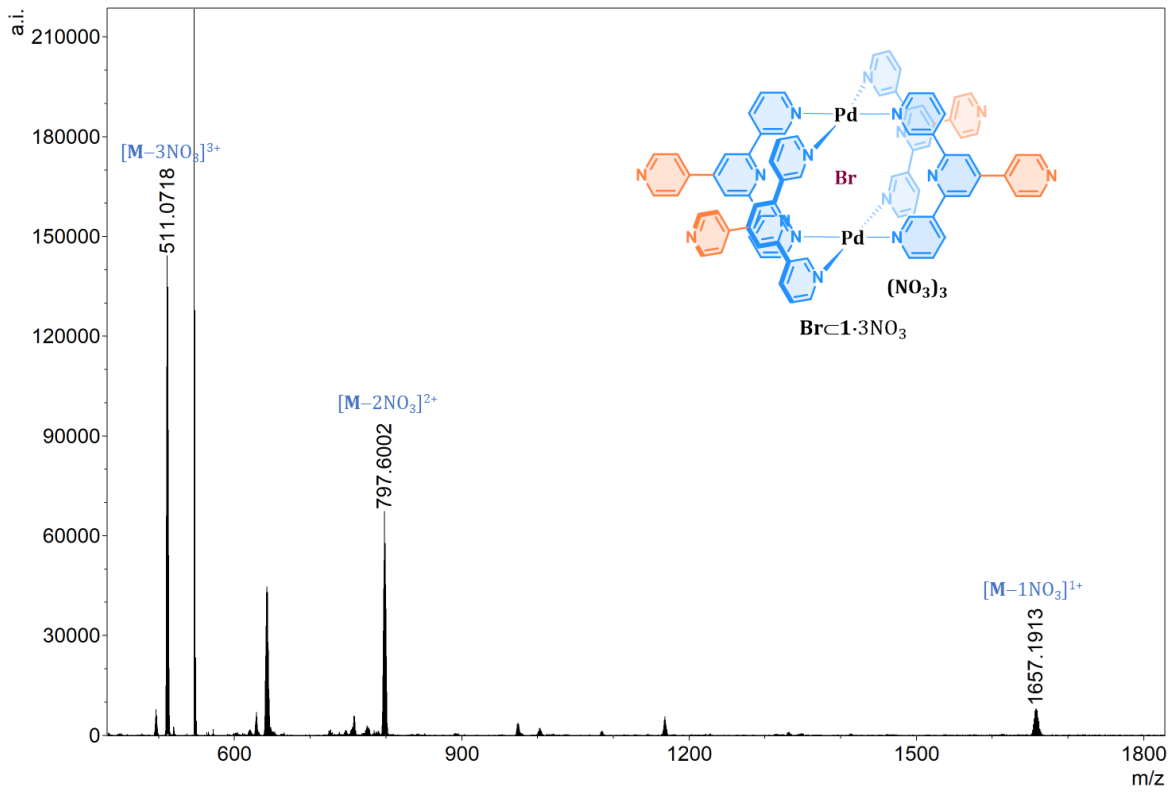


**Figure S22** ESI mass spectral analysis of **Br⊂1**·3$NO_3$.

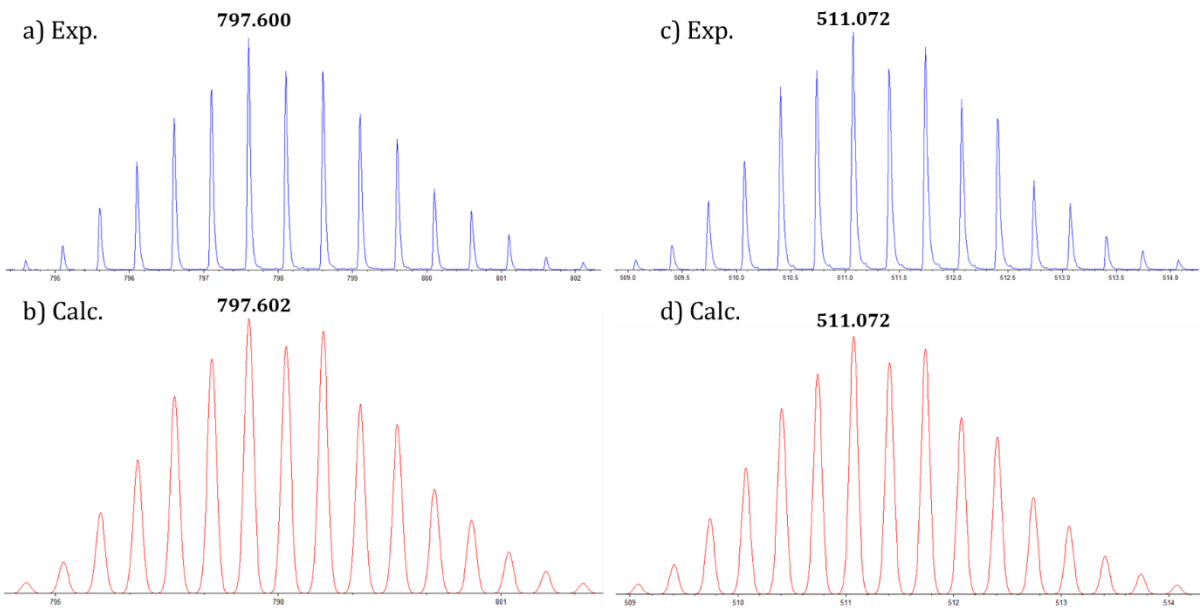


**Figure S23** Experimental (a & c) and theoretical (b & d) isotopic pattern for [**Br⊂1**·3$NO_3$–2$NO_3$]$^{2+}$ and [**Br⊂1**·3$NO_3$–3$NO_3$]$^{3+}$ respectively.

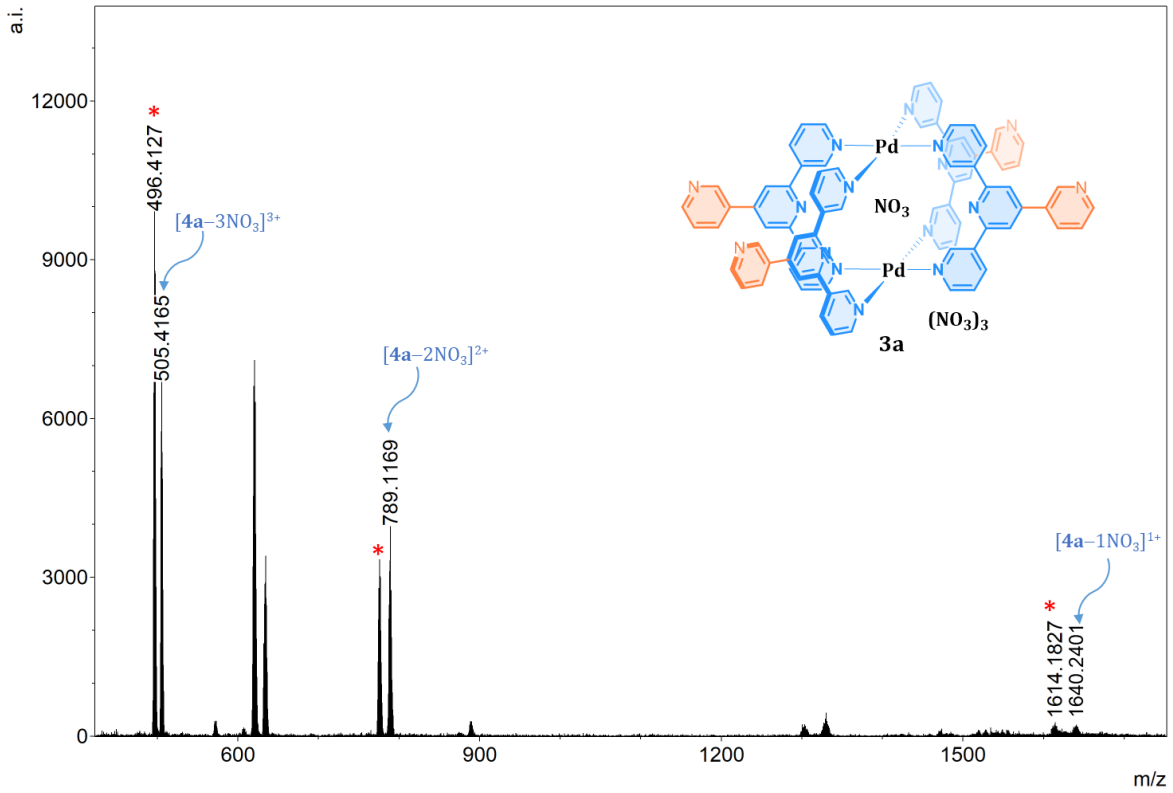


**Figure S24** ESI mass spectral analysis for the mixture containing **$NO_3$⊂3**·3$NO_3$, **3a**. * indicate isotopic patterns corresponds to chloride encapsulated cage **Cl⊂3**·3$NO_3$ (cage sequestrates $Cl^-$ from the environment such as capillary of the instrument, solvents used, etc.).

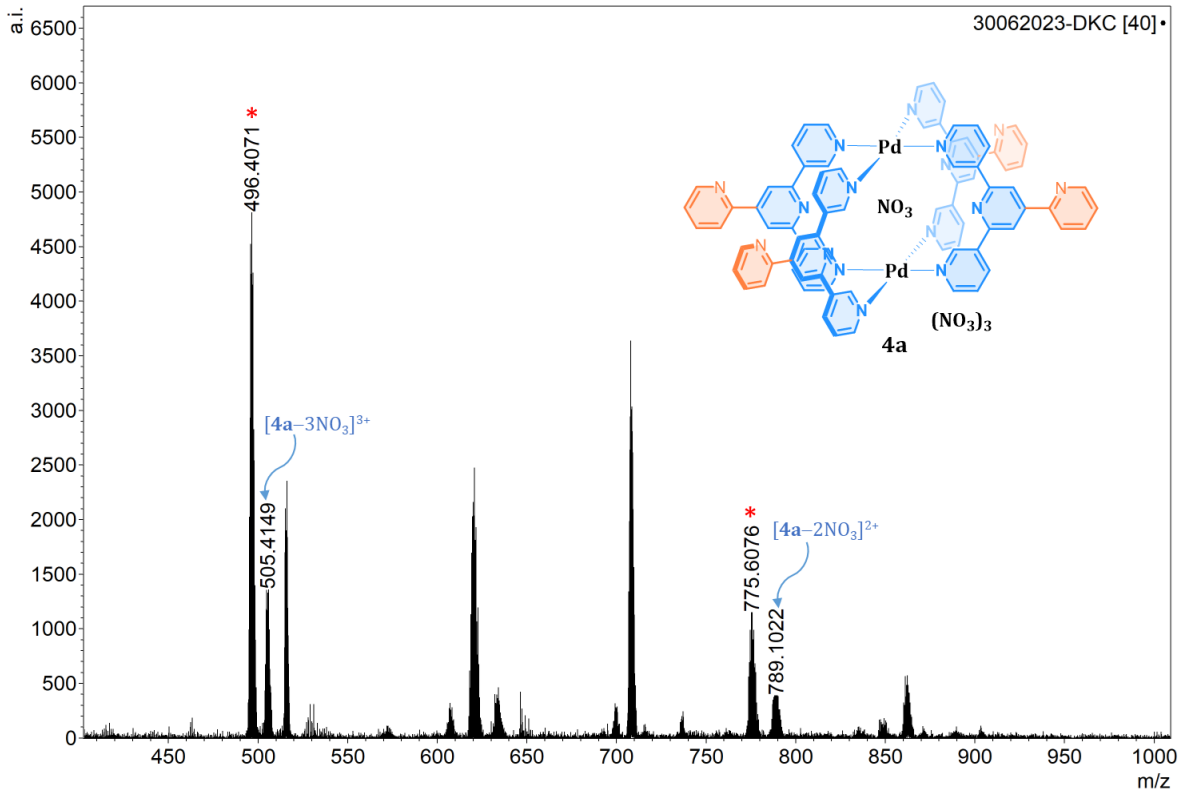


**Figure S25** ESI mass spectral analysis of **$NO_3$⊂4**·3$NO_3$, **4a**. * indicate isotopic patterns corresponds to chloride encapsulated cage **Cl⊂4**·3$NO_3$ (cage sequestrates $Cl^-$ from the environment such as capillary of the instrument, solvents used, etc.).

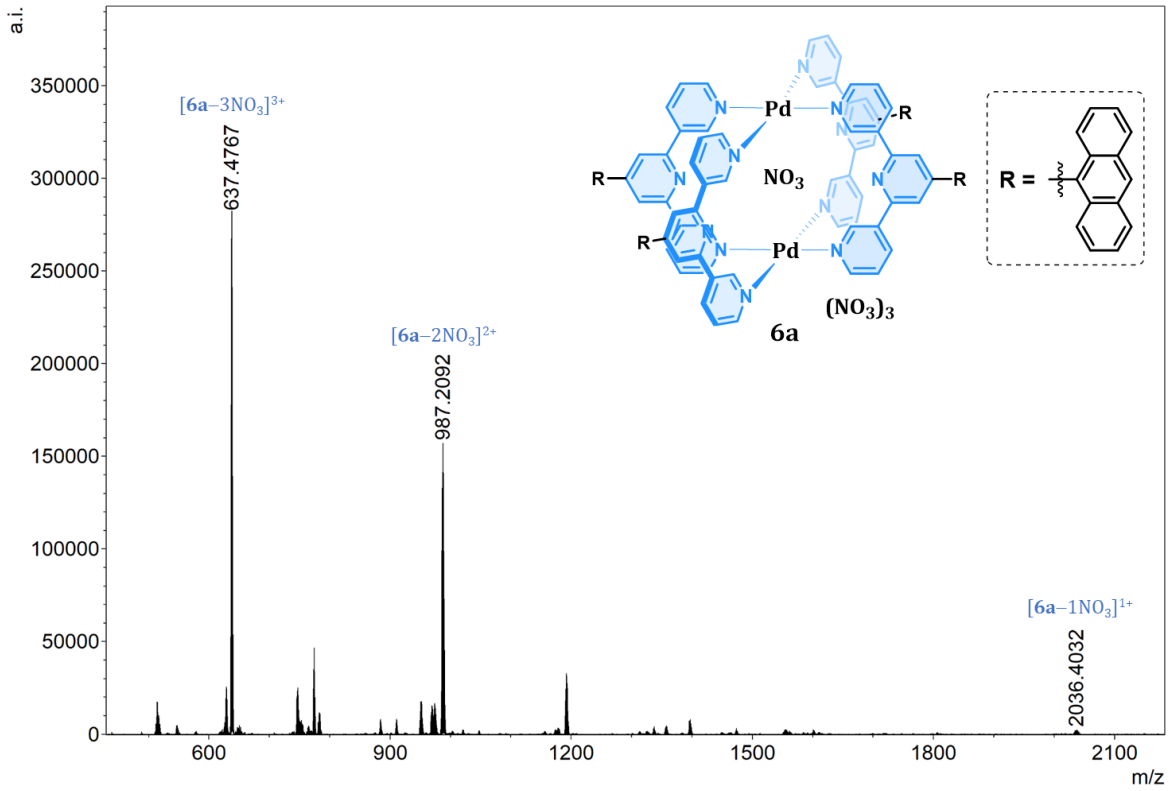


**Figure S26** ESI mass spectral analysis of **$NO_3$⊂6**·3$NO_3$, **6a**.

## 5. Anion exchange studies of $NO_3$⊂**1**·3$NO_3$

### Titration of 1a with TBAF

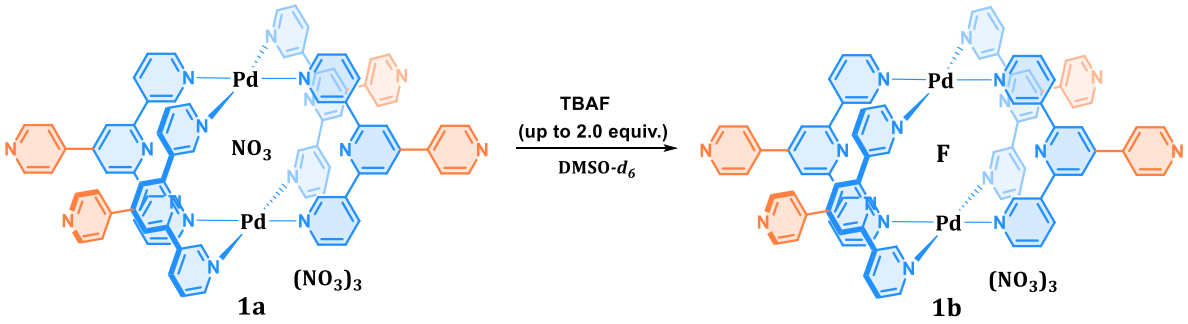


**Scheme S8** Titration of **$NO_3$⊂1**·3$NO_3$ with TBAF (up to 2.0 equiv.).

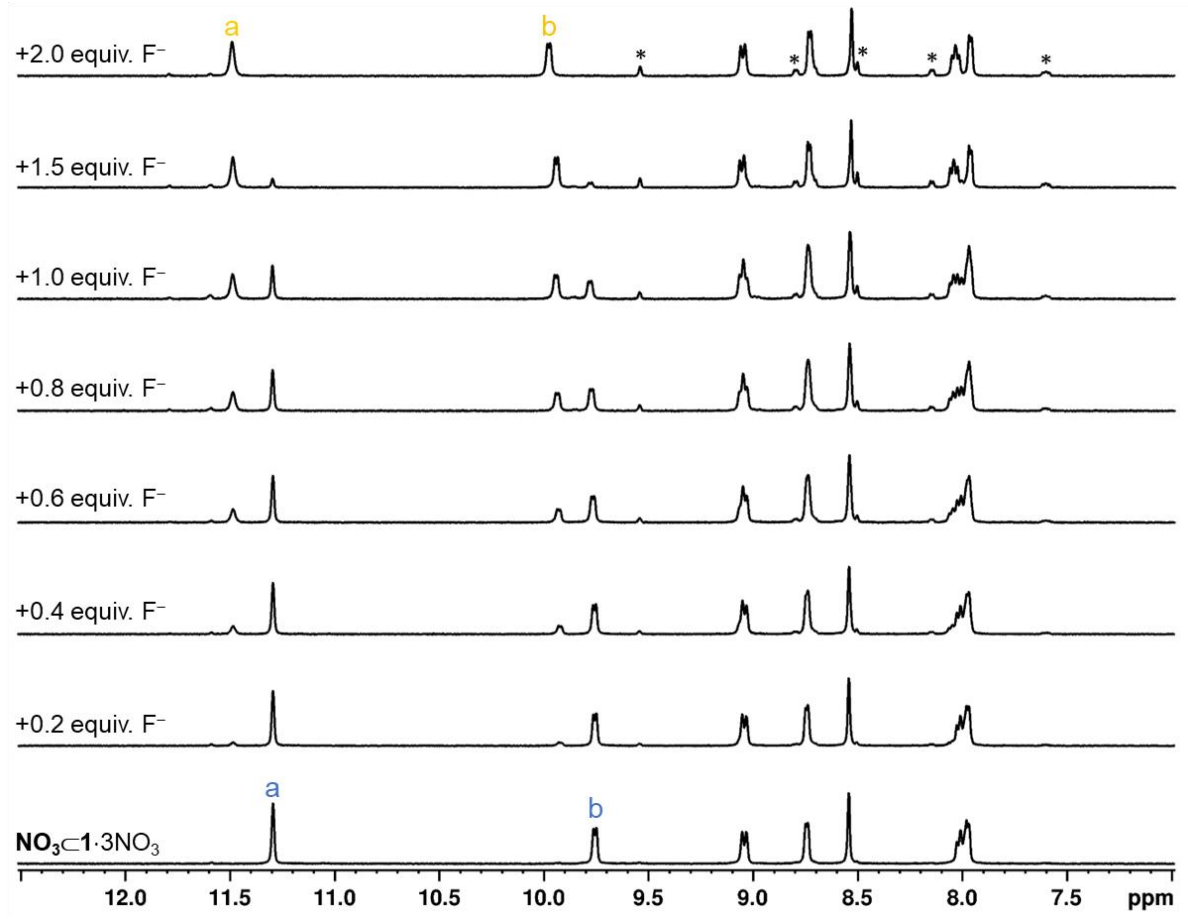


**Figure S27** $^1$H NMR spectra (400 MHz, 298 K) in DMSO-$d_6$ for the titration of **$NO_3$⊂1**·3$NO_3$ with TBAF.

**Titration of 1a with TBACl**


**Scheme S9** Titration of **$NO_3$⊂1**·3$NO_3$ with TBACl (up to 1.0 equiv.).

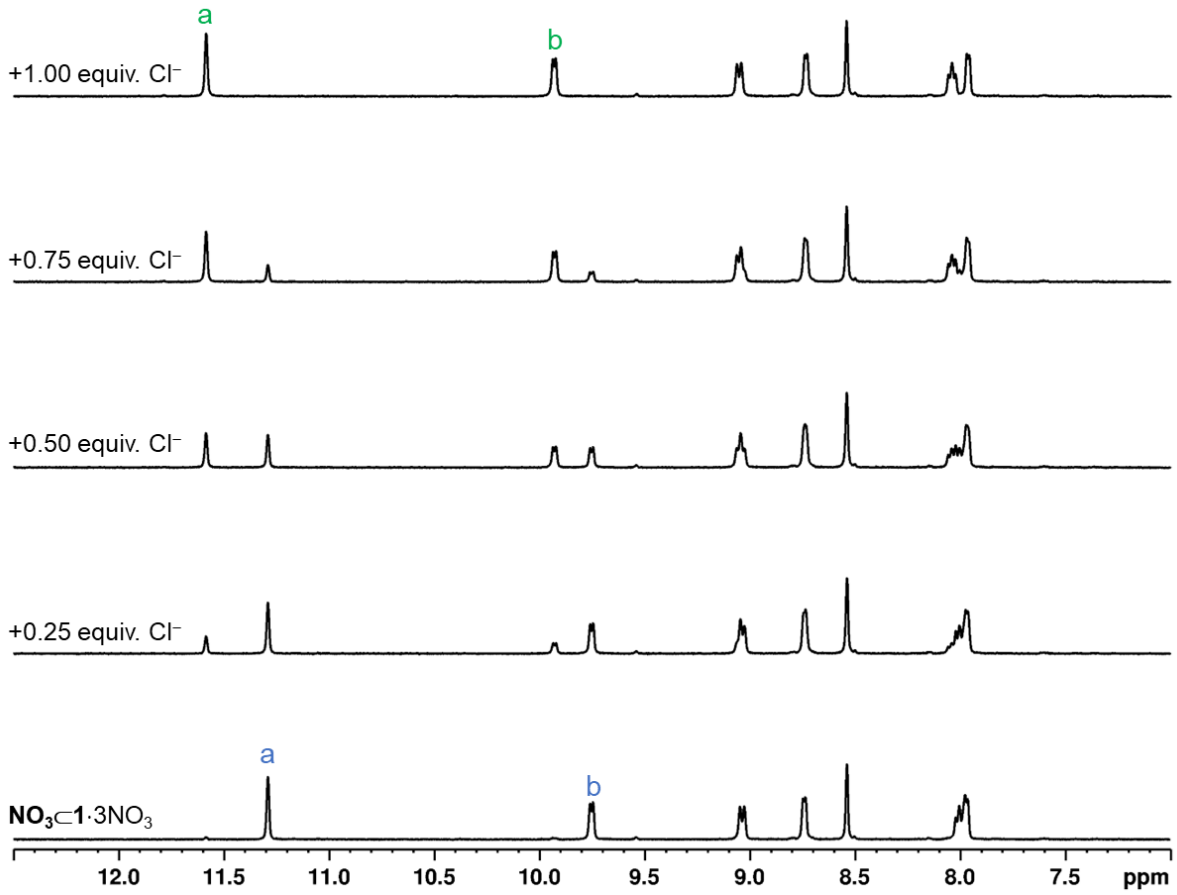


**Figure S28** $^1$H NMR spectra (400 MHz, 298 K) in DMSO-$d_6$ for the titration of **$NO_3$⊂1**·3$NO_3$ with TBACl.

**Titration of 1a with TBABr**

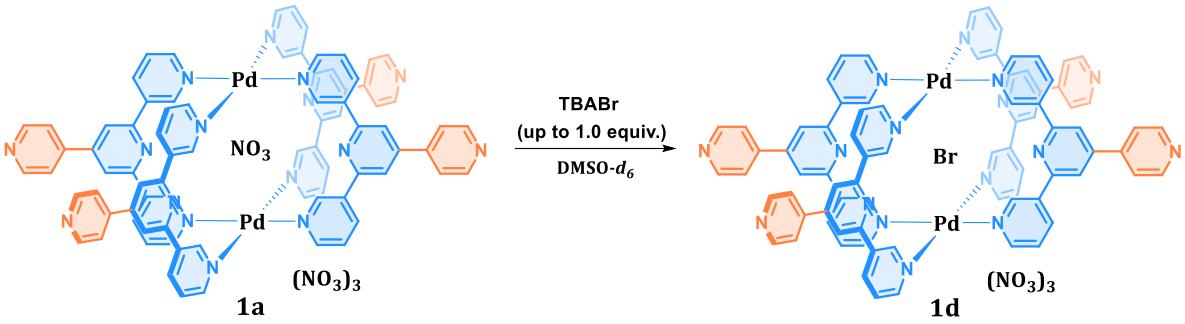


**Scheme S10** Titration of **$NO_3$⊂1**·3$NO_3$ with TBABr (up to 1.0 equiv.).

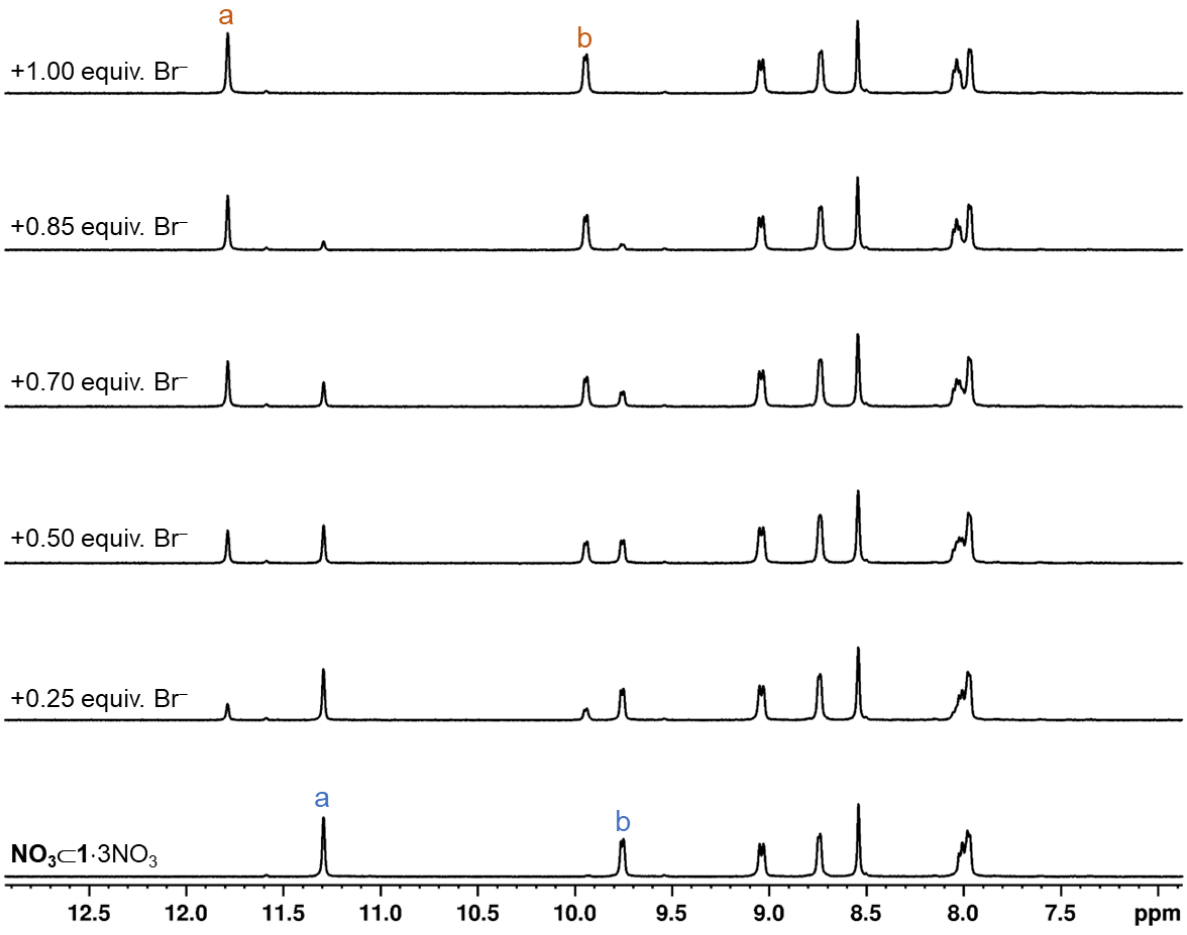


**Figure S29** $^1$H NMR spectra (400 MHz, 298 K) in DMSO-$d_6$ for the titration of **$NO_3$⊂1**·3$NO_3$ with TBABr.

**Titration of 1a with TBAI**

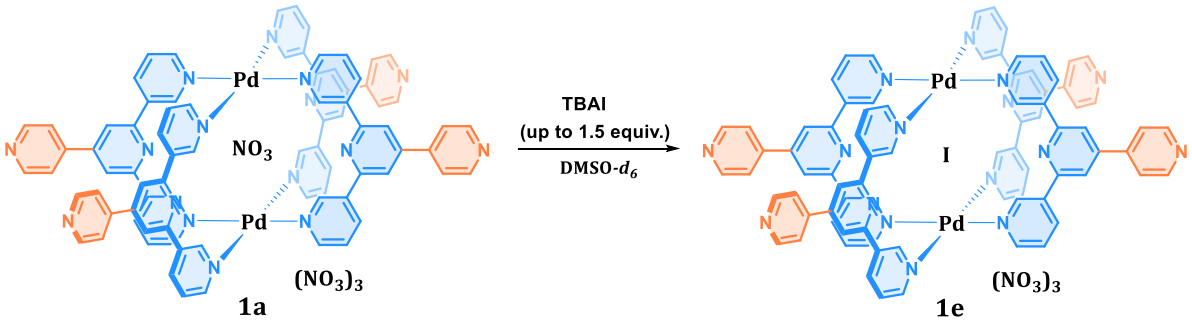


**Scheme S11** Titration of **$NO_3$⊂1**·3$NO_3$ with TBAI (up to 1.5 equiv.).

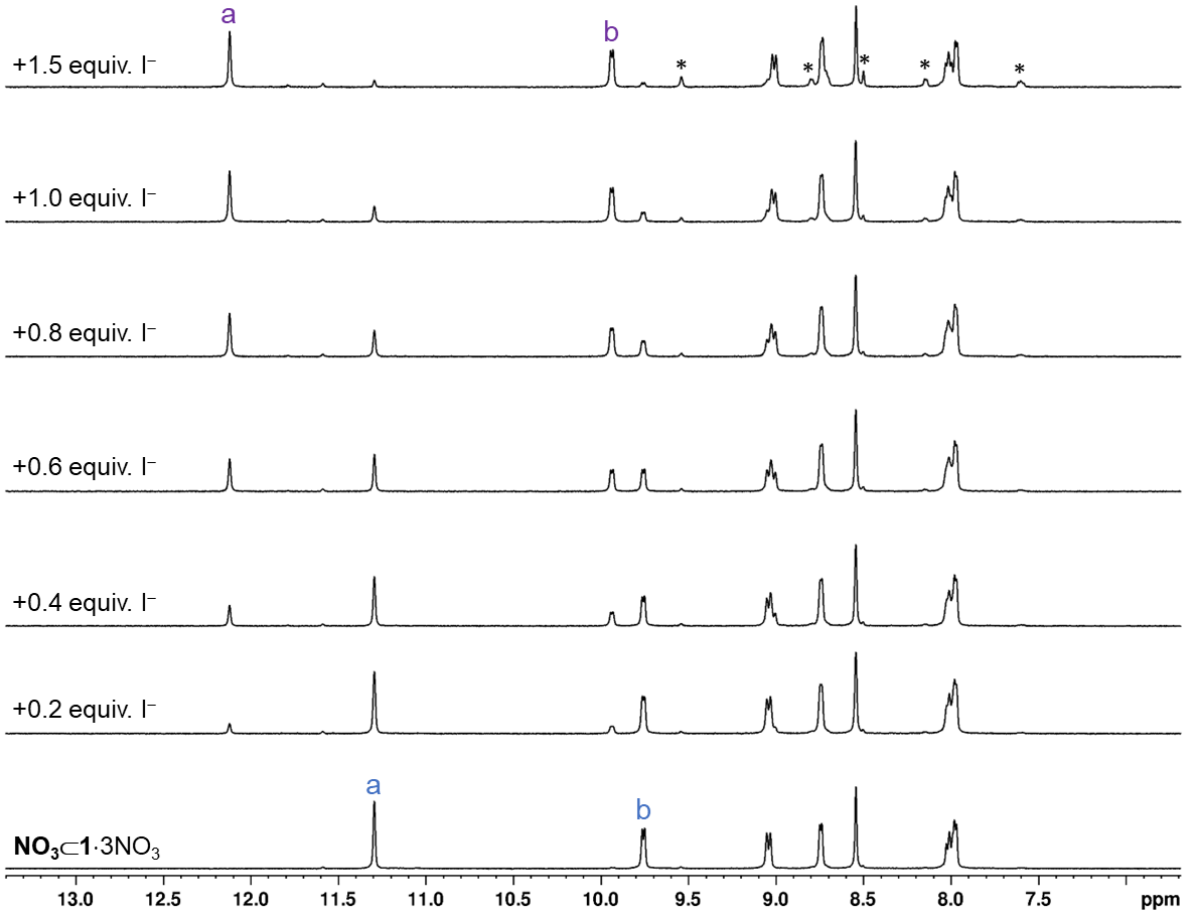


**Figure S30** $^1$H NMR spectra (400 MHz, 298 K) in DMSO-$d_6$ for the titration of **$NO_3$⊂1**·3$NO_3$ with TBAI. * indicate ligand signals

**Complexation of L1 with $Pd(CH_3CN)_4(BF_4)_2$**

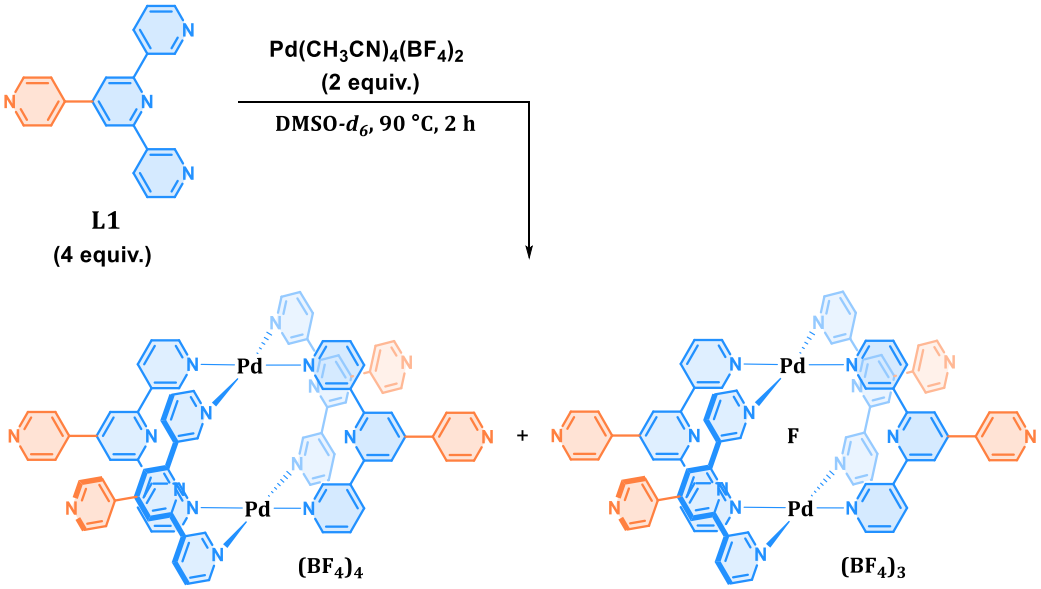


**Scheme S12** Stoichiometry controlled complexation of **L1** with $Pd(CH_3CN)_4(BF_4)_2$ at 4:2 ratio.

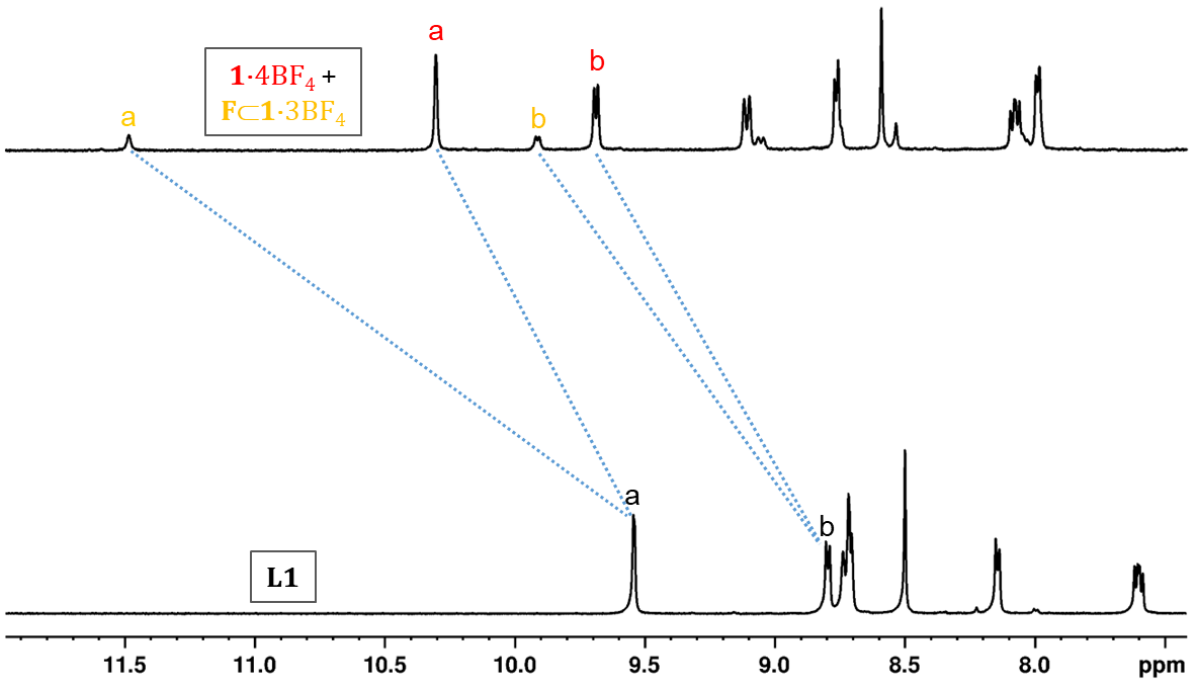


**Figure S31** $^1$H NMR spectra (400 MHz, 298 K) in DMSO-$d_6$ for the complexation of **L1** with $Pd(CH_3CN)_4(BF_4)_2$ at 4:2 ratio (at 90°C for 2 hours).

## 6. Nanosheet assembly and characterization

### Preparation of the metallogel directly from L1

In a glass vial, **L1** (6.21 mg, 0.02 mmol) was dissolved in 0.9 mL of DMSO. To the clear solution, we added 0.1 mL of $Pd(NO_3)_2{\cdot}2H_2O$ (150 mM stock solution) and heated the solution for 30 minutes at 70 °C. The metallogel formation occurred during the heating, then the sample was allowed to cool down to room temperature.

### Preparation of the metallogel from cage, 1a

Cage **1a** (8.51 mg, 0.005 mmol) was dissolved in 0.9 mL of DMSO. To this solution, we added 0.1 mL of $Pd(NO_3)_2{\cdot}2H_2O$ (50 mM stock solution) and stirred for 2 minutes at room temperature. Then, the sample was allowed to stand at room temperature without stirring. A simple vial inversion test confirmed the metallogel formation within 10 minutes. Subsequently, the metallogel can also be successfully prepared in $CH_3CN$:$H_2O$ (1:1) mixture.

### Effect of counteranion on gelation

A fresh $PdX_2$ salt solution (where X = $TsO^-$, $BF_4^-$, $PF_6^-$, $TfO^-$, $MsO^-$ and $ClO_4^-$) was prepared in DMSO by mixing 1 equiv. of $PdCl_2$ and the corresponding AgX salt (2 equiv.) at 70 °C for 30 minutes. In separate glass vials, **L1** (6.21 mg, 0.02 mmol) was dissolved in 0.7 mL of DMSO. To the clear solution, we added 0.3 mL of $PdX_2$ (50 mM in DMSO) was added and heated for 30 minutes at 70 °C. Then the sample was allowed to stand at room temperature. A simple vial inversion test was carried out after 1 hour. We have observed gelation only in the case of $Pd(PF_6)_2$ addition.

### Direct gelation test of ligands L2–L10

Gelation test for the ligands **L2**–**L10** were performed at a constant concentration of 15 mM Pd(II) irrespective of the number of donating sites available in the ligands. In separate glass vials, 0.02 mmol of **L1**/**L2**/**L3**/**L4** or 0.03 mmol of **L5**/**L6** or 0.015 mmol of **L7**/**L8**/**L9**/**L10** were dissolved in 0.9 mL of DMSO. To the clear solution, we added 0.1 mL of $Pd(NO_3)_2{\cdot}2H_2O$ (150 mM stock solution) and the sample was allowed to stand at room temperature for 2 hours. The metallogel formation was confirmed for the samples containing ligands **L1**, **L2**, **L7** and **L10** with a vial inversion test. Other samples were monitored for another 24 hours. Upon failed to form gel those samples were further

heated at 70 °C for 1 hour and then allowed to stand at room temperature for 48 hours. However, no gelation was observed for the samples comprising **L3**, **L4**, **L5**, **L6**, **L8** and **L9** with $Pd(NO_3)_2$.

**Addition of a disulfonate salts to Cage 1a (in DMSO)**

To a 0.45 mL of DMSO solution containing Cage **1a** (4.25 mg, 0.0025 mmol), we added 0.05 mL of 50 mM DMSO solution of a naphthalene-based disulfonate salt (naphthalene-1,5-disulfonate, naphthalene-2,6-disulfonate, naphthalene-2,7-disulfonate) and stirred for 2 minutes at room temperature. Then, the sample was allowed to stand at room temperature without stirring. The mixture turned turbid, but no gelation was observed even after 24 hours.

**Addition of a disulfonate salts to nanosheet assembly (in DMSO)**

To a 0.45 mL of DMSO solution containing nanosheet assembly (i.e., in solution phase below the observed critical gelation concentration; 3 mM $Pd(NO_3)_2$ in 3 mM of cage **1a**), we added 0.05 mL of 30 mM DMSO solution of a naphthalene-based disulfonate salt (naphthalene-1,5-disulfonate, naphthalene-2,6-disulfonate, naphthalene-2,7-disulfonate) and stirred for 2 minutes at room temperature. Then, the sample was allowed to stand at room temperature without stirring. A simple vial inversion test confirmed the metallogel formation within 1 hour for all the three samples. The disulfonate-driven gelation could be due to the aggregation between nanosheet assembly owing to the binding of disulfonate anions towards the pyridine–$\alpha$ protons of Pd(II)-bound 3-pyridyl (outwards pointed) and/or 4-pyridyl units.[5]

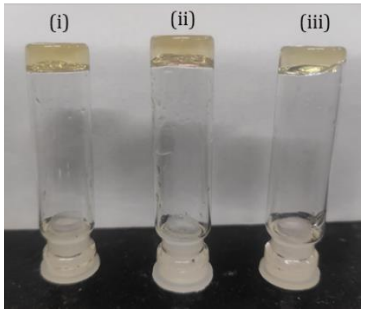


**Figure S32** The gel samples obtained upon addition of i) naphthalene-1,5-disulfonate, ii) naphthalene-2,6-disulfonate, iii) naphthalene-2,7-disulfonate) to the solution containing nanosheet assembly.

**Scanning Electron Microscopy (SEM) images**

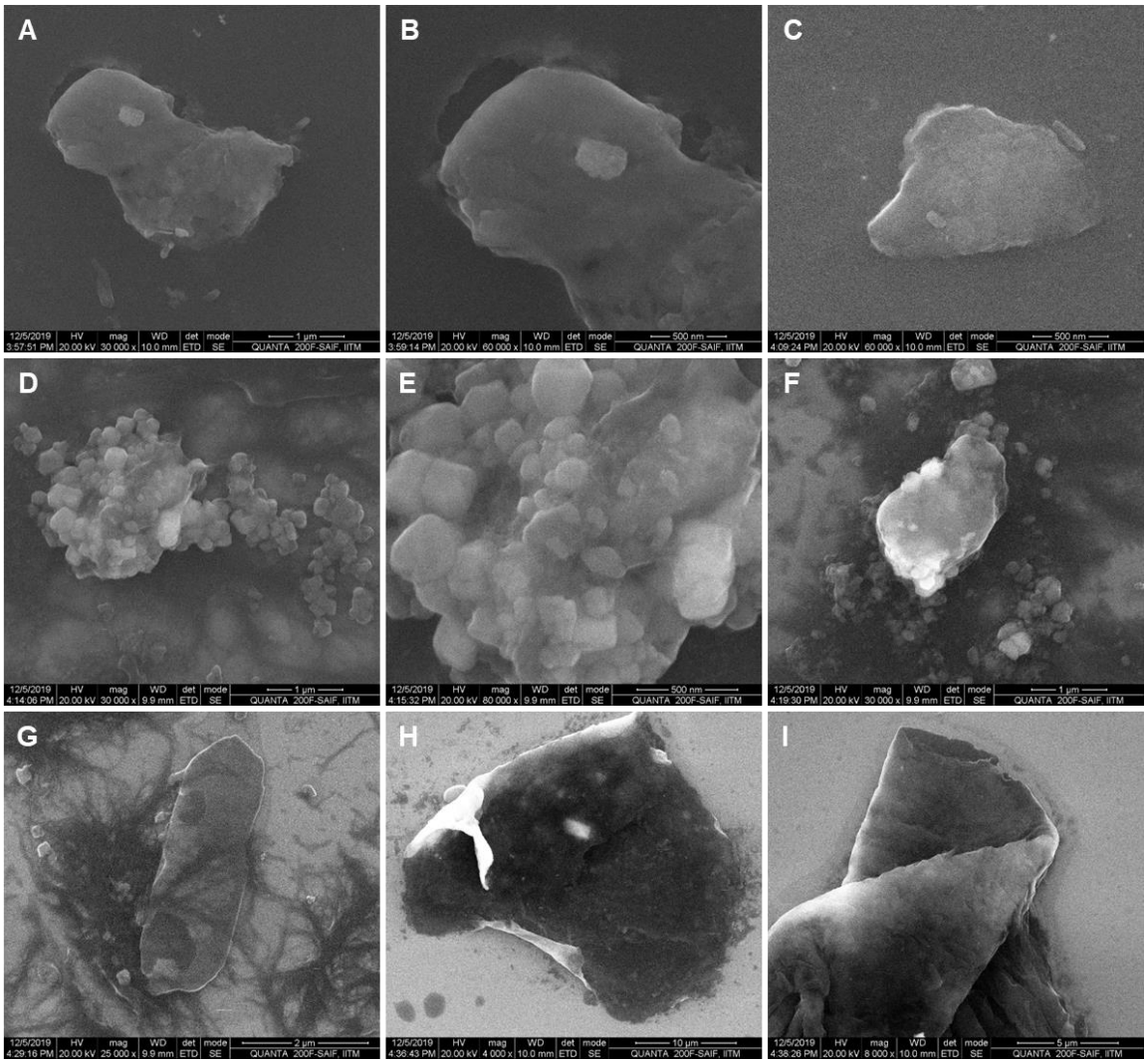


**Figure S33** SEM images of the metallogel samples prepared under different conditions. A–C) The metallogel prepared through a stepwise assembly approach *via* cage **1a**; D–F) the metallogel prepared directly from **L1** (after thermal annealing for 30 minutes at 70 °C); D–F) the metallogel prepared directly from **L1** (after thermal annealing for 2 hours at 90 °C).

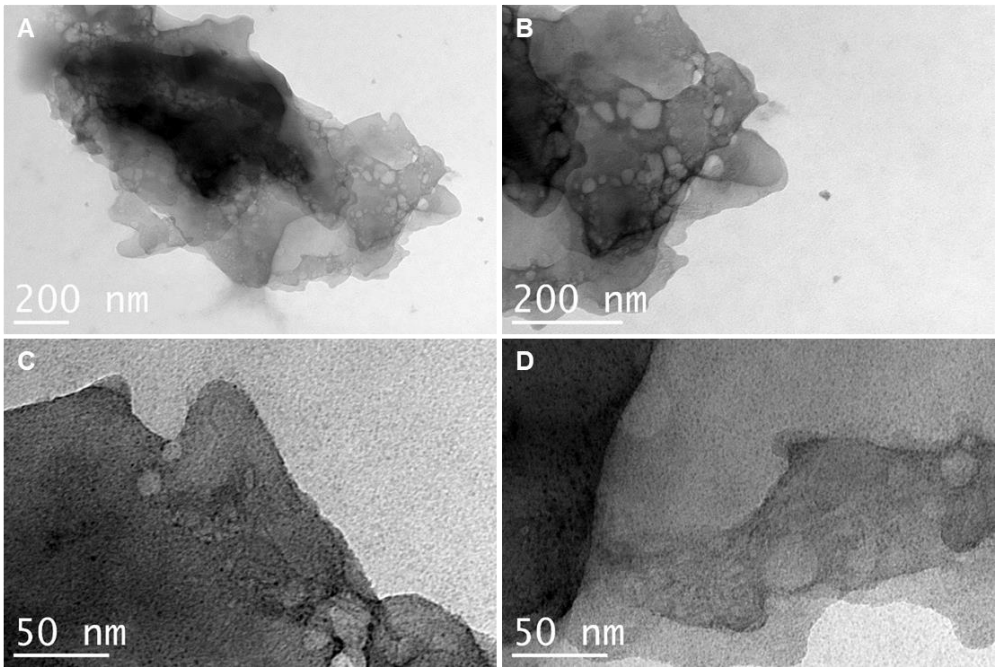


**Figure S34** TEM images of the metallogel sample (15 mM concentration of Pd(II)) prepared through a stepwise assembly approach *via* cage **1a**.

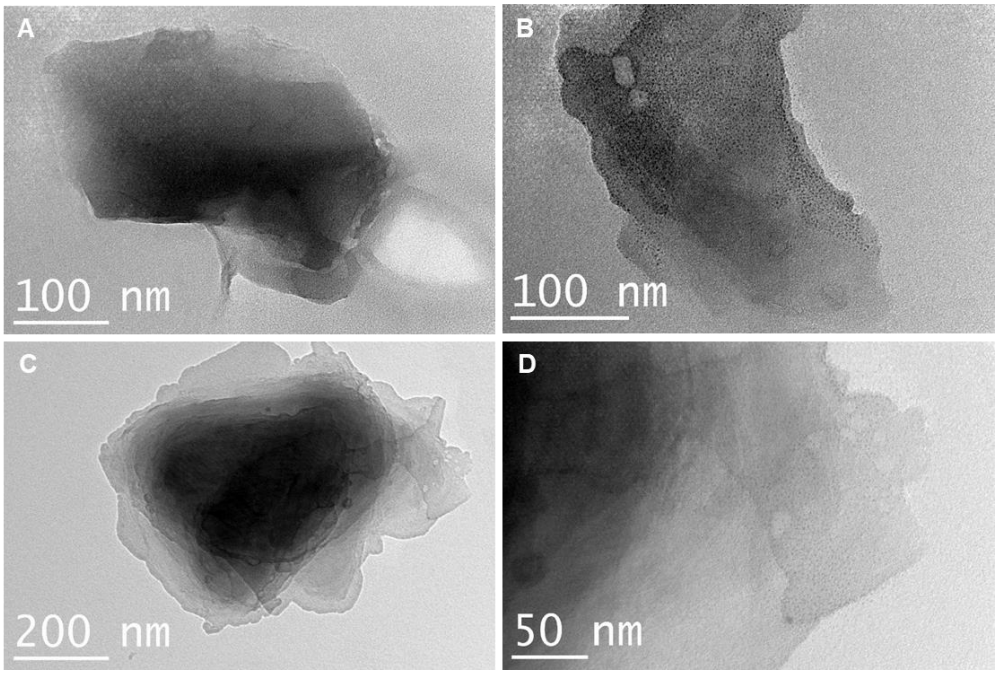


**Figure S35** TEM images of the sample containing the cage-based nanosheet assembly (6 mM concentration of Pd(II)) achieved stepwise *via* cage **1a** (2 mM of cage was used).

**Reversible interconversion between nanosheet assembly and cage 1a**

To a 0.5 mL of metallogel-2 prepared from cage **1a** in DMSO (5 mM $Pd(NO_3)_2$ added to 5 mM of cage **1a**), we added 30 μL of DMAP (1.22 mg) in DMSO. Upon the slow mixing of the sample at room temperature resulted in clear solution. Then, the addition of *p*-toluenesulfonic acid (1.9 mg) turned the solution into gel after 1 hour.

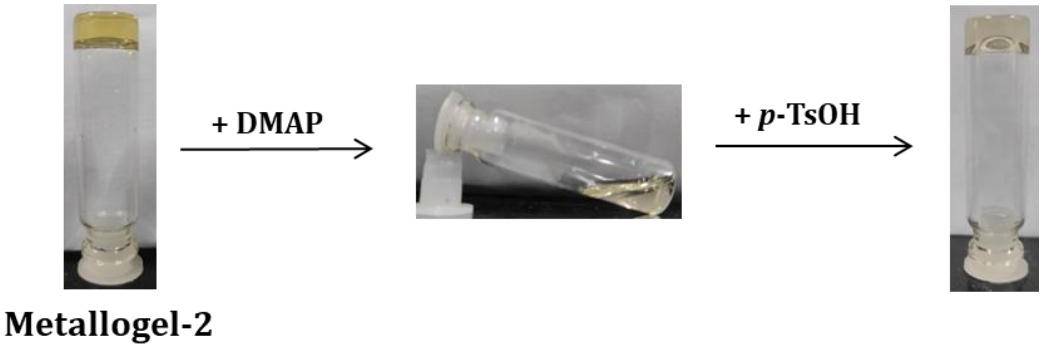


**Figure S36** The Sol-Gel transformation of metallogel-2 for the addition of DMAP followed by *p*-toluenesulfonic acid.

Next, we monitored the reversible transformation between nanosheet assembly and cage **1a** using $^1$H NMR spectroscopy starting with the DMSO-$d_6$ sample containing the nanosheet assembly (2.5 mM of $Pd(NO_3)_2$ in 2.5 mM of cage **1a**). The portion wise addition of DMAP, followed by *p*-toluenesulfonic acid confirms the interconvertible nature of metal-organic cage integrated 2D nanosheets.

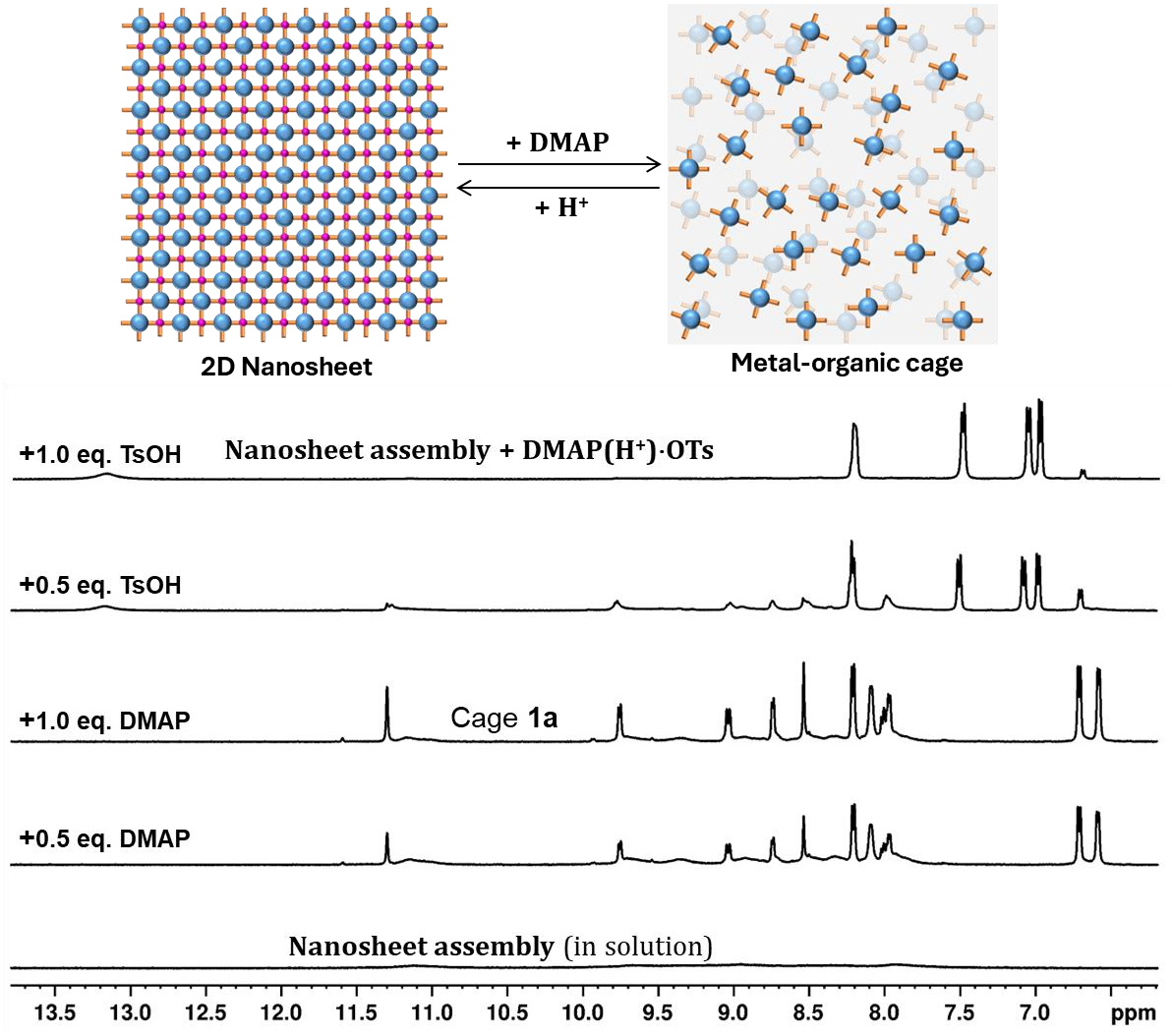


**Figure S37** Schematic illustration and the $^1$H NMR spectra for the interconversion between nanosheet assembly and cage **1a** in DMSO-$d_6$ solution (at 2.5 mM conc. of the cage).

**Dynamic interconversion between cage 2a and oligomeric assembly**

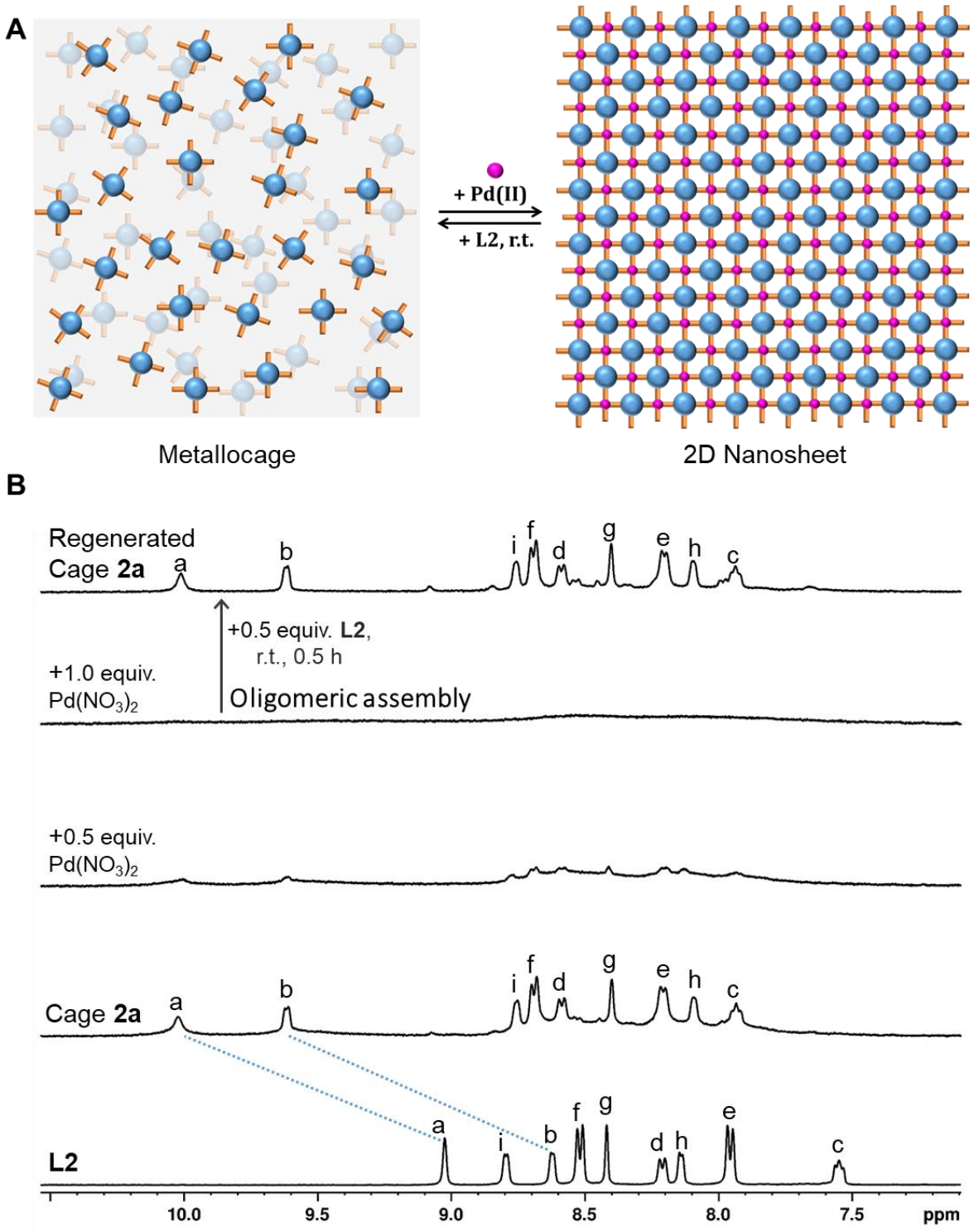


**Figure S38** A) Schematic illustration for the dynamic interconversion between metallocage and 2D nanosheet; B) $^{1}$H NMR spectra for the interconversion between the cage **2a** and oligomeric assembly in DMSO-$d_6$ solution (at 2 mM conc. of the cage).

## References


1. Smith, C. B.; Raston, C. L.; Sobolev, A. N. Poly(ethyleneglycol) (PEG): A Versatile Reaction Medium in Gaining Access to 4′-(pyridyl)-terpyridines. *Green Chem.* **2005**, *7*, 650–654.
2. Granifo, J.; Vargas, M.; Garland, M. T.; Ibáñez, A.; Gaviño, R.; Baggio, R. The Novel Ligand 4′-phenyl-3,2′:6′,3″-terpyridine (L) and The Supramolecular Structure of the Dinuclear Complex $[Zn_2(\mu\text{-}L)(acac)_4]\cdot H_2O$ (acac = acetylacetonato). *Inorg. Chem. Commun*. **2008**, *11*, 1388−1391.
3. Wang, J.; Hanan, G. S. A Facile Route to Sterically Hindered and Non-Hindered 4′-Aryl-2,2′:6′,2″-Terpyridines. *Synlett.* **2005**, 1251–1254.
4. Farha, O. K.; Malliakas, C. D.; Kanatzidis, M. G.; Hupp, J. T. Control over Catenation in Metal−Organic Frameworks via Rational Design of the Organic Building Block. *J. Am. Chem. Soc*. **2010**, *132*, *3*, 950–952.
5. Clever, G. H.; Kawamura, W.; Shionoya, M. Encapsulation versus Aggregation of Metal–Organic Cages Controlled by Guest Size Variation. *Inorg. Chem*. **2011**, *50*, *11*, 4689–4691.